The Ddc2/ATRIP checkpoint protein monitors meiotic recombination intermediates

Esther Refolio[1], Santiago Cavero[1], Edyta Marcon[2], Raimundo Freire[3] and Pedro A. San-Segundo[1,*]

[1]Instituto de Microbiología Bioquímica. CSIC / University of Salamanca, 37007 Salamanca, Spain
[2]Banting and Best Department of Medical Research, University of Toronto, Toronto, ON M5G 1L6, Canada
[3]Hospital Universitario de Canarias, 38320 San Cristobal de la Laguna, Tenerife, Spain
*Author for correspondence (pedross@usal.es)

Accepted 14 March 2011
Journal of Cell Science 124, 2488-2500

doi:10.1242/jcs.081711

Summary

During meiosis, accurate segregation of intact chromosomes is essential for generating healthy gametes. Defects in recombination and/or chromosome synapsis activate the pachytene checkpoint, which delays meiotic cell cycle progression to avoid aberrant chromosome segregation and formation of defective gametes. Here, we characterize the role of the conserved DNA damage checkpoint protein Ddc2/ATRIP in this meiotic surveillance mechanism. We show that deletion of *DDC2* relieves the checkpoint-dependent meiotic block that occurs in *Saccharomyces cerevisiae* mutants defective in various aspects of meiotic chromosome dynamics and results in the generation of faulty meiotic products. Moreover, production of the Ddc2 protein is induced during meiotic prophase, accumulates in checkpoint-arrested mutants and localizes to distinctive chromosomal foci. Formation of meiotic Ddc2 foci requires the generation of Spo11-dependent DNA double-strand breaks (DSBs), and is impaired in an RPA mutant. Chromatin immunoprecipitation analysis reveals that Ddc2 accumulates at meiotic DSB sites, indicating that Ddc2 senses the presence of meiotic recombination intermediates. Furthermore, pachytene checkpoint signaling is defective in the *ddc2* mutant. In addition, we show that mammalian ATRIP colocalizes with ATR, TopBP1 and RPA at unsynapsed regions of mouse meiotic chromosomes. Thus, our results point to an evolutionary conserved role for Ddc2/ATRIP in monitoring meiotic chromosome metabolism.

Key words: Meiosis, Checkpoint, Recombination, Ddc2, ATRIP

Introduction

Eukaryotic cells possess surveillance mechanisms, generally referred to as DNA integrity checkpoints, which promote and coordinate an adequate cellular response to the presence of lesions in the genome. These checkpoint pathways are composed of sensors that detect the damage and transmit the signal to the checkpoint effectors through a series of molecular events. In turn, the effectors act on the target proteins eliciting the various cellular responses to face genome injuries, depending on the nature of the DNA damage or the cell cycle phase when it occurred.

Meiosis is a special type of cell division that generates haploid gametes from diploid parental cells. One of the particularities of meiosis is that it implies the deliberate introduction of double-strand breaks (DSBs) by the conserved Spo11 protein (Keeney et al., 1997) to initiate meiotic recombination, which is essential for the proper distribution of chromosomes to the meiotic progeny. Therefore, although meiotic DSBs can be considered as physiological or programmed DNA damage, there are also meiosis-specific surveillance mechanisms, collectively known as the meiotic recombination checkpoint or pachytene checkpoint, devoted to monitor different aspects of the progression of this crucial meiotic event.

During meiotic prophase, the pairing, synapsis and recombination between homologous chromosomes (homologs) result in physical links connecting them (chiasmata), which contribute to the correct orientation on the meiosis I spindle and the subsequent segregation of homologs to opposite poles. At meiosis II, sister chromatids separate to generate haploid nuclei, which are normally encapsidated in specialized cellular structures forming the gametes (Roeder, 1997; Petronczki et al., 2003). In yeast, the meiotic products are enclosed in spores containing thick cell walls to resist harsh environmental conditions. In response to defects in chromosome synapsis and/or recombination, the pachytene checkpoint is triggered and blocks entry into meiosis I to prevent aberrant chromosome segregation and the formation of defective gametes (Roeder and Bailis, 2000; Borner, 2006; Hochwagen and Amon, 2006; Longhese et al., 2009). In humans, aneuploidy resulting from meiotic errors is the main cause of spontaneous miscarriages, birth defects and infertility disorders (Hassold and Hunt, 2001).

Several components of the pachytene checkpoint have been identified in *Saccharomyces cerevisiae*, including 'mitotic' DNA damage checkpoint proteins such as Mec1, Rad24 and the 9-1-1 complex (Lydall et al., 1996; Hong and Roeder, 2002); nucleolar-enriched proteins such as Pch2 and Fpr3 (San-Segundo and Roeder, 1999; Hochwagen et al., 2005); histone modifiers such as Dot1 and Sir2 (San-Segundo and Roeder, 1999; San-Segundo and Roeder, 2000); and meiosis-specific chromosomal proteins such as Mek1, Red1 and Hop1 (Bailis et al., 2000; Woltering et al., 2000; Wan et al., 2004; Carballo et al., 2008; Eichinger and Jentsch, 2010). The meiotic cell cycle delay imposed by the checkpoint is brought about by Swe1-dependent inhibitory phosphorylation of Cdc28 (the budding yeast cyclin-dependent kinase) at tyrosine 19 (Leu and Roeder, 1999), and by inhibition of the Ndt80 transcription factor, which controls the induction of expression of a subset of meiotic genes involved in meiosis I entry (Chu and Herskowitz, 1998; Tung et al., 2000; Pak and Segall, 2002), the most relevant target being the gene encoding the polo-like kinase Cdc5 (Sourirajan and Lichten, 2008).

Journal of Cell Science

Defects in various aspects of meiotic recombination and/or chromosome metabolism trigger checkpoint-dependent delay or arrest of meiotic progression, which suggests that different types of aberrant recombination intermediates or chromosome structures can be sensed by the meiotic checkpoints (Hochwagen and Amon, 2006). Thus, yeast mutants, such as *zip1*, *dmc1*, *hop2* and *sae2*, showing different types of meiotic defects, are useful tools for studying the pachytene checkpoint. Zip1 is the major component of the central region of the synaptonemal complex (SC), which is an elaborate proteinaceous structure holding homologs together (synapsis) during the pachytene stage of meiotic prophase. Therefore, in *zip1* mutants, homologs fail to synapse (Sym et al., 1993). In addition, *zip1* mutants are also defective in crossovers formation (Borner et al., 2004). The Dmc1 protein is a meiosis-specific RecA homolog involved in the strand-exchange reaction of meiotic recombination; thus, *dmc1* mutants accumulate unrepaired resected DSBs (Bishop et al., 1992). The Hop2 protein, forming a complex with Mnd1, facilitates Dmc1-dependent meiotic interhomolog recombination and *hop2* cells also fail to repair DSBs (Tsubouchi and Roeder, 2002; Tsubouchi and Roeder, 2003; Chen et al., 2004; Henry et al., 2006). In addition, the *hop2* mutant shows non-homologous synapsis (Leu et al., 1998). The Sae2/Com1 protein participates in meiotic recombination during DSB resection; that is, at an earlier step than Dmc1 and Hop2. In the *sae2/com1* mutant, Spo11 remains bound to the ends of the DSB, preventing DNA resection (Keeney et al., 1997; McKee and Kleckner, 1997; Prinz et al., 1997).

Although the meiotic recombination checkpoint pathway has been extensively studied in budding yeast, meiotic surveillance mechanisms are conserved throughout evolution, operating also in fission yeast (Shimada et al., 2002; Perez-Hidalgo et al., 2003), worms (Bhalla and Dernburg, 2005), flies (Joyce and McKim, 2009) and mammals (de Rooij and de Boer, 2003). In particular, knockout male mice lacking structural components of the SC (i.e. SCP3/SCYP3) or deficient in proteins directly involved in meiotic DSB repair (i.e. Dmc1) display a sterility phenotype due to a gametogenesis block and apoptotic elimination of the arrested spermatocytes (Pittman et al., 1998; Yuan et al., 2000). The analysis of meiotic checkpoint proteins in mammals has been difficult due to the inviability or to the severe sickness of mutants defective in putative components of this checkpoint that also play roles in somatic cells. Nevertheless, cytological studies are consistent with a function for checkpoint proteins, such as ATR, TopBP1 and Rad1, in meiotic surveillance mechanisms (Keegan et al., 1996; Freire et al., 1998; Moens et al., 1999; Perera et al., 2004; Barchi et al., 2005).

The budding yeast Mec1–Ddc2 complex plays a key role in the DNA damage response (Harrison and Haber, 2006) and, although Ddc2 localization and recruitment has been extensively used as marker for the presence of DNA damage in vegetative yeast cells, little was known about its functional implication in meiosis. To gain further understanding of the meiotic recombination checkpoint we report here a thorough functional study of the *S. cerevisiae* Ddc2 protein and a cytological analysis of its mammalian homolog, ATRIP. We characterize the pachytene checkpoint defects of *ddc2* mutants and describe the localization of Ddc2 to distinctive foci representing meiotic recombination intermediates. Furthermore, the localization of ATRIP in mouse spermatocytes supports an evolutionary conserved role for Ddc2/ATRIP in sensing meiotic defects.

Results

Ddc2 is required for the pachytene checkpoint

To investigate the meiotic role of the conserved Ddc2/ATRIP checkpoint proteins, we carried out a functional study of budding yeast Ddc2 (also known as Lcd1/Pie1). Because *DDC2* is an essential gene in *S. cerevisiae*, deletion of *DDC2* was made in a *sml1* mutant background, which allows the *ddc2* mutant to live but does not alter its DNA damage checkpoint defect (Paciotti et al., 2000). To discard any possible meiotic effect of the lack of Sml1, we first verified that the *sml1* single mutant progressed through meiosis with wild-type kinetics (supplementary material Fig. S1A) and produced a high proportion of viable spores (>85%). By contrast, although the *sml1 ddc2* double mutant also progressed normally through meiosis (supplementary material Fig. S1A), it showed reduced spore viability (27%), indicative of a role for Ddc2 in an otherwise unperturbed meiosis. Moreover, the lack of Sml1 had no or little effect on the checkpoint-mediated prophase arrest or delay of the *zip1*, *dmc1* or *hop2* meiotic mutants tested (supplementary material Fig. S1B–D). Thus, for simplicity, *sml1 ddc2* strains will be referred to as *ddc2* throughout this paper.

To determine whether Ddc2 is required for the pachytene checkpoint, we combined deletion of *DDC2* with mutations, such as *zip1*, *dmc1*, *hop2* and *sae2*, that confer meiotic defects at different steps in the recombination and/or synapsis processes and trigger checkpoint-dependent meiotic arrest or delay (see Introduction). Several meiotic events were analyzed in all these mutants (Fig. 1, Fig. 2A, supplementary material Figs S2, S3). In particular, the kinetics of meiotic nuclear division were monitored by DAPI staining of nuclei and, in some cases, following spindle elongation. Dityrosine fluorescence was used as a specific indicator for the presence of mature spores, whereas sporulation efficiency, assessed by microscopic scoring of asci, represents the formation of either mature of immature asci. Finally, spore viability, which reflects the fidelity of meiotic chromosome segregation and the integrity of the spore genome, was determined by tetrad dissection.

As expected, the *zip1* mutant displayed a robust pachytene arrest (Sym et al., 1993) that was completely alleviated in *zip1 ddc2* strains, resulting in formation of four-spore mature asci with apparently intact nuclei in most cases (Fig. 1A,C, supplementary material Fig. S2). However, the spore viability of *zip1 ddc2* was significantly reduced and the pattern of spore death changed compared with that of the few meiotic products formed in the *zip1* single mutant after prolonged incubation in sporulation medium (Fig. 1A,B).

In BR strains of budding yeast, the *dmc1* mutant shows a significant meiotic delay due to activation of the pachytene checkpoint (Rockmill et al., 1995), but eventually undergoes meiosis and sporulation, forming mature dityrosine-containing spores (Fig. 1A,D, Fig. 2A, supplementary material Fig. S3). Nonetheless, spore viability of *dmc1* was low. Deletion of *DDC2* suppressed the *dmc1* meiotic delay, but the meiotic nuclei appeared broken and disorganized, and few mature spores, mostly inviable, were formed (Fig. 1A,D, Fig. 2A, supplementary material Fig. S3). We interpret this to mean that, during the checkpoint-imposed meiotic delay in *dmc1*, some DSBs could be eventually repaired using the sister chromatid instead of the homolog as a donor. This would result in the formation of intact chromosomes and the generation of mature, though largely inviable, spores due to chromosome missegregation in the absence of interhomolog connections. However, if the meiotic delay of *dmc1* were abolished by *ddc2*, cells would undergo meiotic divisions with unrepaired

DSBs, resulting in fragmented nuclei unable to promote proper spore morphogenesis. To test this possibility, we introduced a *rad54* mutation, which impairs sister-chromatid recombination (Arbel et al., 1999). The *rad54* single mutant did not show a significant meiotic delay and spore viability was not strongly affected, but the *rad54 dmc1* double mutant displayed a tighter meiotic block, consistent with the accumulation of DSBs that cannot be repaired with either sisters or homologs. Furthermore, this meiotic block was alleviated in *rad54 dmc1 ddc2*, which led to the formation of defective meiotic products (Fig. 1A,E, supplementary material Fig. S3).

As seen for *dmc1*, DSBs remain unrepaired in the *hop2* mutant but, in addition, there is extensive synapsis between nonhomologous chromosomes resulting in a robust pachytene checkpoint-dependent prophase arrest (Leu et al., 1998). Interestingly, this arrest was relieved when *DDC2* was deleted, leading to immature asci and inviable spores (Fig. 1A,F, Fig. 2A, supplementary material Fig. S2, supplementary material Fig. S3B,C).

In the *sae2* mutant, the presence of unrepaired unresected DSBs also triggers a meiotic checkpoint, resulting in a delayed meiotic progression (Wu and Burgess, 2006) (Fig. 1G), although *sae2* eventually sporulated to some extent and produced dead spores (Fig. 1A). The *ddc2 sae2* double mutant exhibited faster kinetics of meiotic progression and higher sporulation efficiency compared with *sae2*, but spores were still inviable and showed aberrant distribution of genetic material (Fig. 1A,G, supplementary material Fig. S2). Thus, Ddc2 is required for the meiotic arrest or delay of mutants defective in synapsis and/or recombination.

In the absence of Ddc2, cells undergo meiotic divisions with unrepaired DSBs

The fact that mutation of *DDC2* bypasses the checkpoint-dependent prophase arrest/delay of several meiotic mutants and leads to the formation of defective meiotic products strongly suggests that Ddc2 is a crucial component of the pachytene checkpoint. To confirm that the absence of Ddc2 relieves the dependence between two meiotic cell cycle events (completion of recombination and entry into meiosis I), we monitored Rad51 foci, as a marker for meiotic recombination intermediates, and tubulin staining to follow meiotic spindle elongation on chromosome spreads (Lydall et al., 1996; San-Segundo and Roeder, 2000). As expected, *hop2* showed numerous Rad51 foci representing unrepaired DSBs, and the spindle did not elongate because pachytene checkpoint activation prevented entry into meiosis I (Fig. 2B). In the wild type, Rad51 foci were only present during prophase, indicative of ongoing recombination (Fig. 2B); however, in meiosis I cells 23 out of 25 wild-type meiosis I nuclei examined contained

A

Relevant genotype	Dityrosine fluorescence	Sporulation efficiency (%)	Spore viability (%)
wild type		63	96.2
zip1		6	44.0
zip1 ddc2		50	6.9
dmc1		29	10.4
dmc1 ddc2		36	3.5
rad54		66	60.4
rad54 dmc1		13	11.1
rad54 dmc1 ddc2		26	3.5
hop2		7	0.7
hop2 ddc2		39	0
sae2		33	0
sae2 ddc2		52	0

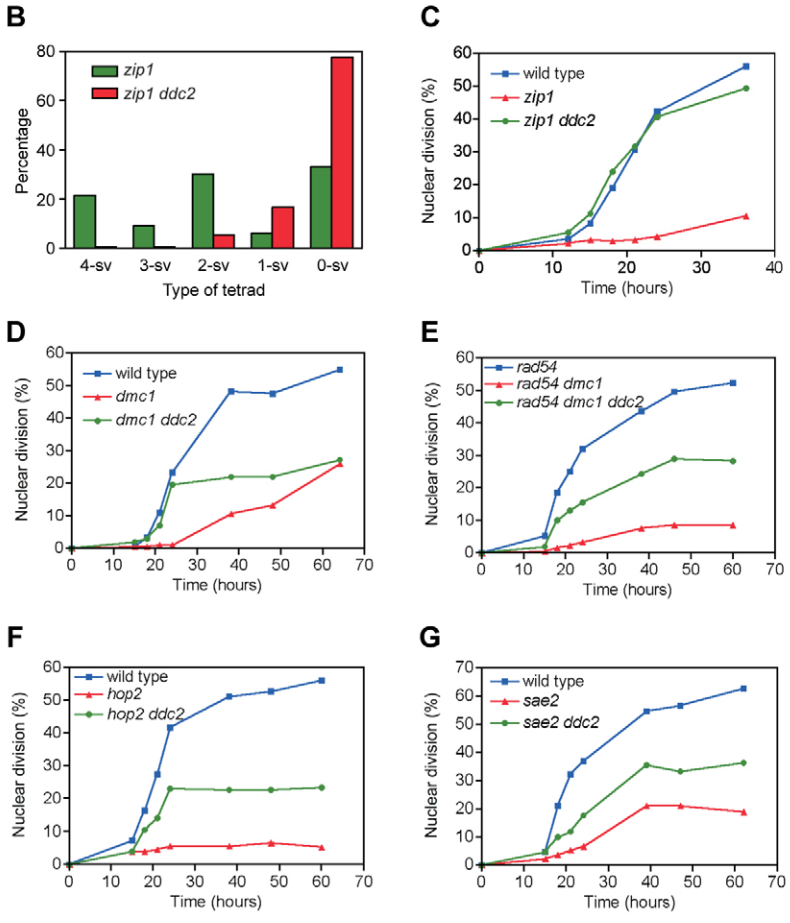

Fig. 1. Ddc2 is required for checkpoint-induced meiotic arrest of the *zip1*, *dmc1*, *hop2* and *sae2* mutants. (**A**) Dityrosine fluorescence, sporulation efficiency and spore viability were examined after 3 days of sporulation on plates. (**B**) Distribution of tetrad types. The percentage of tetrads with 4, 3, 2, 1 and 0 viable spores (4-sv, 3-sv, 2-sv, 1-sv and 0-sv, respectively) is represented. (**C–G**) Time course of meiotic nuclear divisions. The percentage of cells containing more than two nuclei is represented. At least 300 cells were scored for each strain at each time point. Strains are BR1919-2N (wild type), DP452 (*zip1*), DP451 (*zip1 ddc2*), DP467 (*dmc1*), DP468 (*dmc1 ddc2*), DP473 (*rad54*), DP475 (*rad54 dmc1*), DP481 (*rad54 dmc1 ddc2*), DP471 (*hop2*), DP472 (*hop2 ddc2*), DP485 (*sae2*) and DP489 (*sae2 ddc2*).

no Rad51 signal, and only two nuclei showed a single focus. By contrast, the *hop2 ddc2* double mutant entered meiosis I despite the presence of recombination intermediates, and many Rad51 strong foci (an average of 18.1±5.1) coexisted with the meiosis I, and even the meiosis II, spindle in all 28 nuclei examined (Fig. 2B). The same phenotype (i.e. presence of Rad51 foci together with meiosis I or meiosis II spindles) was observed in *dmc1 ddc2* (Fig. 2C). Therefore, Ddc2 is required for the checkpoint that prevents meiotic chromosome segregation until recombination has been completed.

Ddc2 is required for pachytene checkpoint signaling

To further delineate the function of Ddc2 in the pachytene checkpoint, we monitored downstream molecular events in the checkpoint pathway, such as activation of the Mek1 effector kinase and inhibition of the Ndt80-dependent production of Cdc5. As shown in Fig. 2D, the *dmc1*-induced hyperphosphorylation of the effector kinase Mek1 was abolished in the absence of Ddc2, despite the presence of unrepaired DSBs (Fig. 2C). As a control, mutation of *SPO11* also resulted in deficient Mek1 activation because DSBs are not formed. Moreover, the *dmc1 ddc2* mutant was also defective in signaling to the terminal checkpoint targets; whereas induction of Cdc5 was delayed in the *dmc1* mutant, in agreement with its slow meiotic progression (Fig. 1D, Fig. 2A), *dmc1 ddc2* displayed the same timing of Cdc5 induction as wild-type or *dmc1 spo11* cells (Fig. 2D). Thus, Ddc2 functions at an early step in the pachytene checkpoint pathway, signaling the presence of meiotic recombination intermediates to downstream components.

Ddc2 is induced during meiosis and accumulates in pachytene-checkpoint arrested mutants

To study protein levels and localization of Ddc2 during meiosis, the *DDC2* gene was tagged at the genomic locus with either the green fluorescent protein (GFP), or three copies of the hemagglutinin (HA) epitope. Both tagged proteins are functional because they did not confer sensitivity to the genotoxic agent

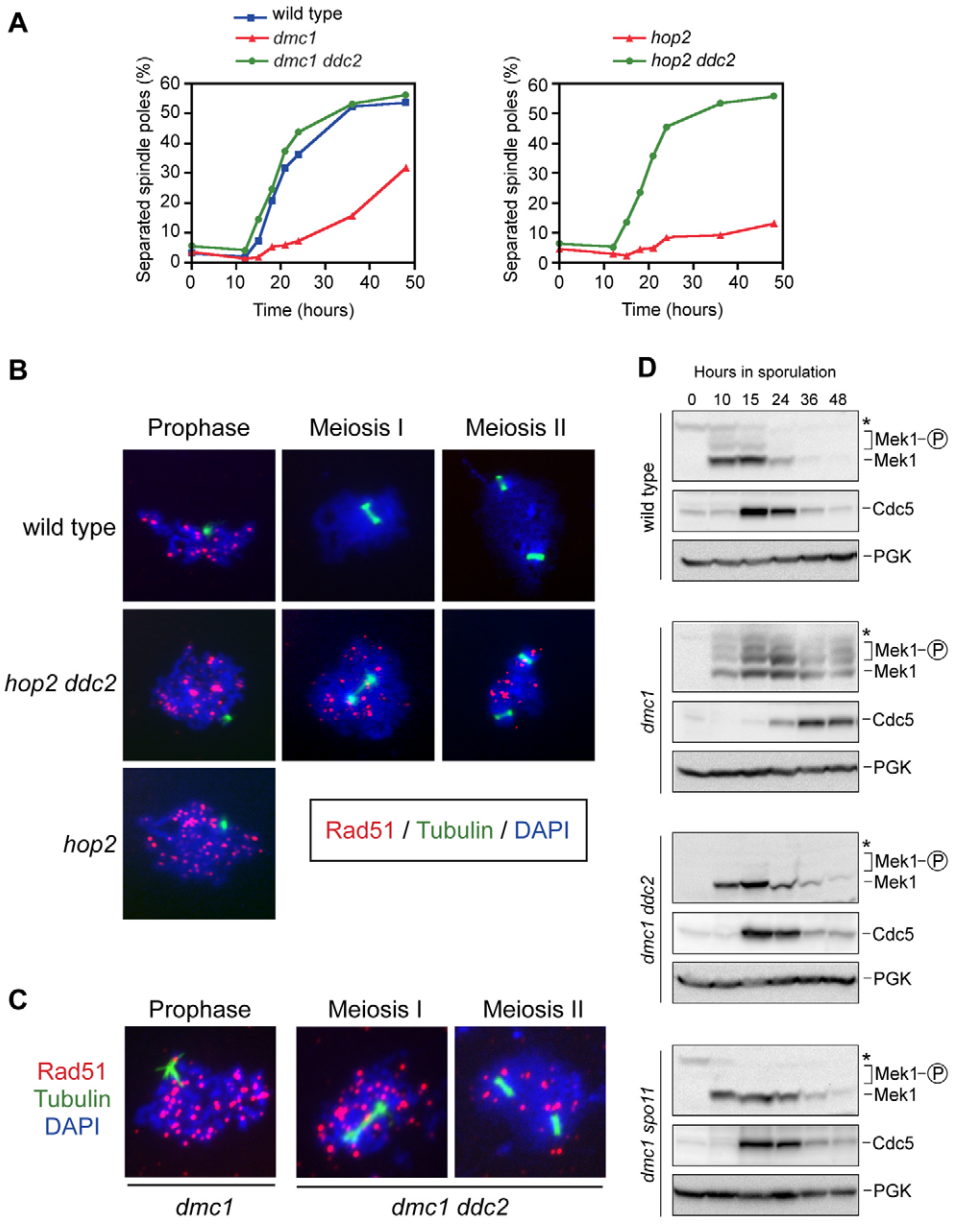

Fig. 2. Ddc2 prevents meiotic chromosome segregation in the presence of recombination intermediates. (**A**) Analysis of spindle pole separation in wild-type (DP778), *dmc1* (DP779), *dmc1 ddc2* (DP781), *hop2* (DP780) and *hop2 ddc2* (DP782) strains expressing GFP-tagged tubulin. Between 150 and 400 cells were scored for each strain at each time point. (**B**,**C**) Spread meiotic nuclei stained with DAPI (blue), and anti-Rad51 (red) and anti-tubulin (green) antibodies. Representative images of each meiotic stage are shown. Strains are BR1919-2N (wild type), DP471 (*hop2*), DP472 (*hop2 ddc2*), DP467 (*dmc1*) and DP468 (*dmc1 ddc2*). (**D**) Western blot analysis of Mek1 activation and Cdc5 induction in wild-type (DP455), *dmc1* (DP467), *dmc1 ddc2* (DP468) and *dmc1 spo11* (DP466) strains. PGK was used as a loading control. The Mek1 gel contained Phos-tag to resolve the phosphorylated bands. The asterisk marks a nonspecific band.

methyl methanesulfonate (MMS) (data not shown), they did not alter the meiotic arrest or delay of the *zip1*, *dmc1*, *hop2* and *sae2* mutants (supplementary material Fig. S4), and they supported high levels of spore viability (92% and 96% for otherwise wild-type *DDC2-GFP* and *DDC2-HA* strains, respectively). When we analyzed Ddc2 levels throughout meiosis by western blot, we observed that a faint Ddc2 band was detected in wild-type vegetative cells (0 hours); then, Ddc2 levels increased during meiotic prophase (around 12–18 hours) and declined gradually as meiotic divisions and sporulation occurred (Fig. 3A). As a control, we also analyzed the levels of the well-characterized meiosis-specific Mek1 kinase, which is produced during meiotic prophase (Rockmill and Roeder, 1991). As shown in Fig. 3A, Ddc2 and Mek1 displayed the same meiotic expression profile, except that low levels of Ddc2 were detected in vegetative cells and in spores, consistent with its role in the DNA damage checkpoint in mitotic cells. By contrast, when the pachytene checkpoint was triggered in the *zip1*, *dmc1*, *hop2* or *sae2* mutants, the Ddc2 protein remained for a longer time and/or accumulated to higher levels after inducing meiosis (Fig. 3B). Thus, Ddc2 production rises during meiotic prophase and accumulates in checkpoint-arrested mutants.

Phosphorylation of Ddc2 at the [S/T]Q Mec1 consensus sites is not required for checkpoint function

In vegetative cells, DNA damage triggers Mec1-dependent phosphorylation of Ddc2 (Paciotti et al., 2000). Ddc2 contains three consensus sites, [S/T]Q, for phosphorylation by Mec1 at threonines 29 and 40, and serine 636. To investigate the relevance of phosphorylation at these sites for checkpoint function, we mutated them to alanine in a centromeric plasmid containing *DDC2* tagged with the myc epitope (Rouse and Jackson, 2002), creating the *ddc2-3AQ* allele. To determine whether Ddc2 phosphorylation at these sites is required for the pachytene checkpoint, we analyzed meiotic progression in the *zip1 ddc2* diploid transformed with the empty vector or plasmids expressing either wild-type *DDC2* or the *ddc2-3AQ* mutant. As controls, wild-type and *zip1* strains transformed with empty vector were also included (Fig. 3C). Although plasmid-expressed *DDC2-myc* only partially restored the meiotic arrest to *zip1 ddc2* (due to plasmid-loss events), the kinetics of meiotic progression was indistinguishable from that of *zip1 ddc2* transformed with the *ddc2-3AQ* allele (Fig. 3C). Likewise, we did not observe differences between *DDC2* and *ddc2-3AQ* in other meiotic mutants tested (data not shown), indicating that phosphorylation of Ddc2 at amino acids 29, 40 and 636 is not required for pachytene checkpoint function.

We also analyzed the DNA damage response in vegetative cells. We found that, in contrast to *ddc2Δ*, the *ddc2-3AQ* mutant was not sensitive to the genotoxic agents MMS and UV irradiation (supplementary material Fig. S5A), and MMS-induced activation of Rad53 was not impaired (supplementary material Fig. S5B),

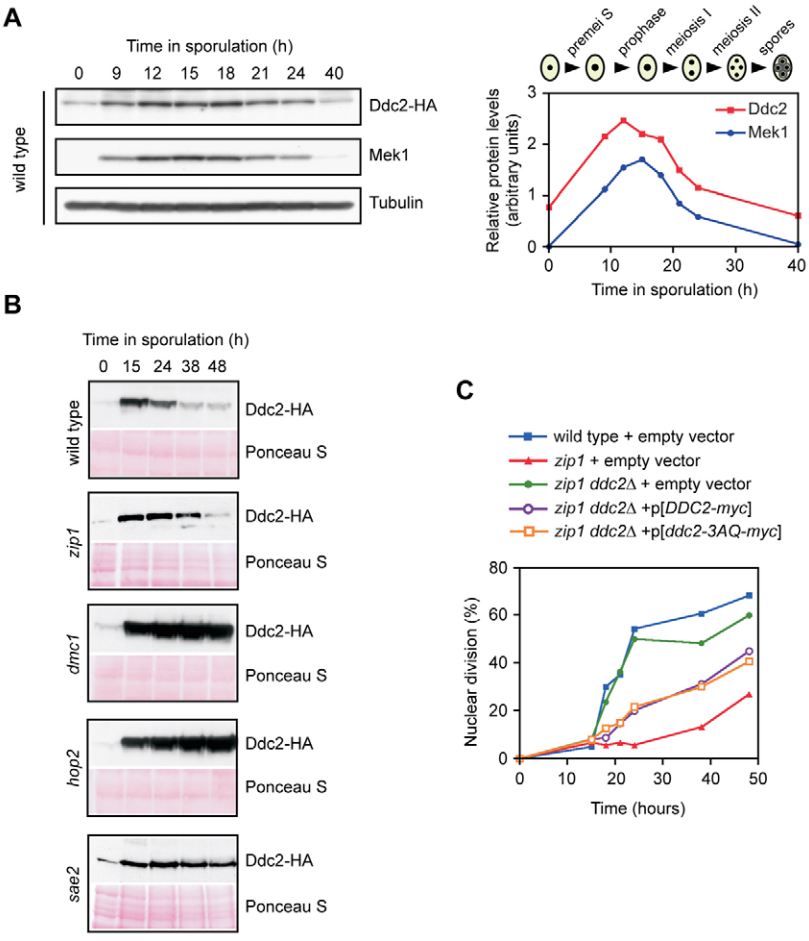

Fig. 3. Analysis of meiotic production and phosphorylation of Ddc2. (**A**) Left: Western blot analysis of Ddc2–HA and Mek1 throughout meiosis in a wild-type strain (DP697). Tubulin was used as loading control. Right: Quantification of the Ddc2 and Mek1 relative levels, normalized to tubulin, is shown. The approximate timing of key meiotic events in BR strains is depicted. (**B**) Ddc2 accumulates in checkpoint-arrested mutants. Western blot analysis of Ddc2–HA throughout meiosis in wild-type (DP487), *zip1* (DP490), *dmc1* (DP488), *hop2* (DP491) and *sae2* (DP492) strains. Ponceau S staining of the membranes is shown as a loading control. (**C**) Phosphorylation of Ddc2 at the [S/T]Q Mec1 consensus sites is dispensable for its meiotic checkpoint function. Graph shows a time course of meiotic nuclear divisions. The percentage of cells containing more than two nuclei is represented. Strains are DP455 + pRS316 (wild type), DP452 + pRS316 (*zip1*), DP451 + pRS316 (*zip1 ddc2Δ*), DP451 + pLCD1-MYC (*zip1 ddc2Δ* + p[*DDC2-myc*]) and DP451 + pSS136 (*zip1 ddc2Δ* + p[*ddc2-3AQ-myc*]).

indicating that phosphorylation of Ddc2 at the consensus sites for Mec1 is also dispensable for the DNA damage checkpoint.

Ddc2 localizes to meiotic chromosomes and accumulates in mutants that trigger the pachytene checkpoint

To further investigate the role of Ddc2 during meiosis, localization of the HA- or GFP-tagged protein was examined by immunofluorescence on surface-spread meiotic chromosomes. In the wild type, Ddc2 localized to discrete foci that were more numerous during zygotene (as assessed by Zip1 staining) and decreased or disappeared by pachytene, when most DSBs are repaired (Fig. 4). Strikingly, in mutants deficient in meiotic DSB repair, such as *hop2* or *dmc1*, Ddc2 foci accumulated dramatically during meiotic prophase (Fig. 4, supplementary material Fig. S6), suggesting that Ddc2 localizes at sites of ongoing recombination. Double staining for Ddc2 and Rad51 showed a partial, but significant ($P<0.0001$), colocalization of these two proteins on chromosome spreads from the *hop2* and *dmc1* mutants (supplementary material Fig. S7).

Next, we studied the meiotic dynamics of Ddc2 localization in living cells expressing *DDC2-GFP*. In the wild-type strain, as well as in the meiotic mutants, a small proportion of cells displayed Ddc2 foci at time zero, probably arising from spontaneous damage generated during the mitotic growth prior to meiotic induction (Fig. 5). In the wild type, the number of cells with Ddc2–GFP foci increased as the cells entered the meiotic program, reaching maximum levels coincident with the prophase period when meiotic recombination occurs; then, the fraction of foci-containing cells decreased as meiotic divisions were completed and spores formed (Fig. 5A). By contrast, in the *zip1*, *hop2*, *sae2* and *dmc1* meiotic mutants tested, the fraction of cells showing Ddc2–GFP foci rose to higher levels, accumulating during the meiotic time course (Fig. 5A,B).

Moreover, a detailed examination of Ddc2–GFP localization revealed different foci patterns during meiosis. At time zero, most cells with Ddc2–GFP signal displayed a single bright focus (Fig. 6), similar to those developed in response to DNA damage (Lisby et al., 2004). However, as cells entered the meiotic program, another pattern of Ddc2 localization consisting of multiple small foci often arranged in thread-like structures was observed. Remarkably, although in the wild-type strain this organization of Ddc2 foci declined as meiosis progressed, in the *zip1* mutant a substantial fraction of cells with multiple Ddc2 foci remained at late time points and, in the case of the *dmc1*, *hop2* or *sae2* mutants, defective in meiotic DSB repair, the majority of cells displayed numerous Ddc2 foci at late meiosis (Fig. 6).

Altogether, these observations suggest that the individual Ddc2 foci present at the earlier time points likely represent spontaneous damage occurring during pre-meiotic growth and/or during premeiotic DNA replication. By contrast, the multiple foci observed transiently in the wild type and accumulating in the mutants reflect the presence of Ddc2 at the sites of programmed meiotic DSBs. To further explore this possibility, we examined the Ddc2–GFP signal in the absence of meiotic recombination, that is, in *spo11* or *spo11 dmc1* live cells. Strikingly, in *spo11*, the threads of multiple Ddc2 foci were completely absent and the Ddc2–GFP signal was only

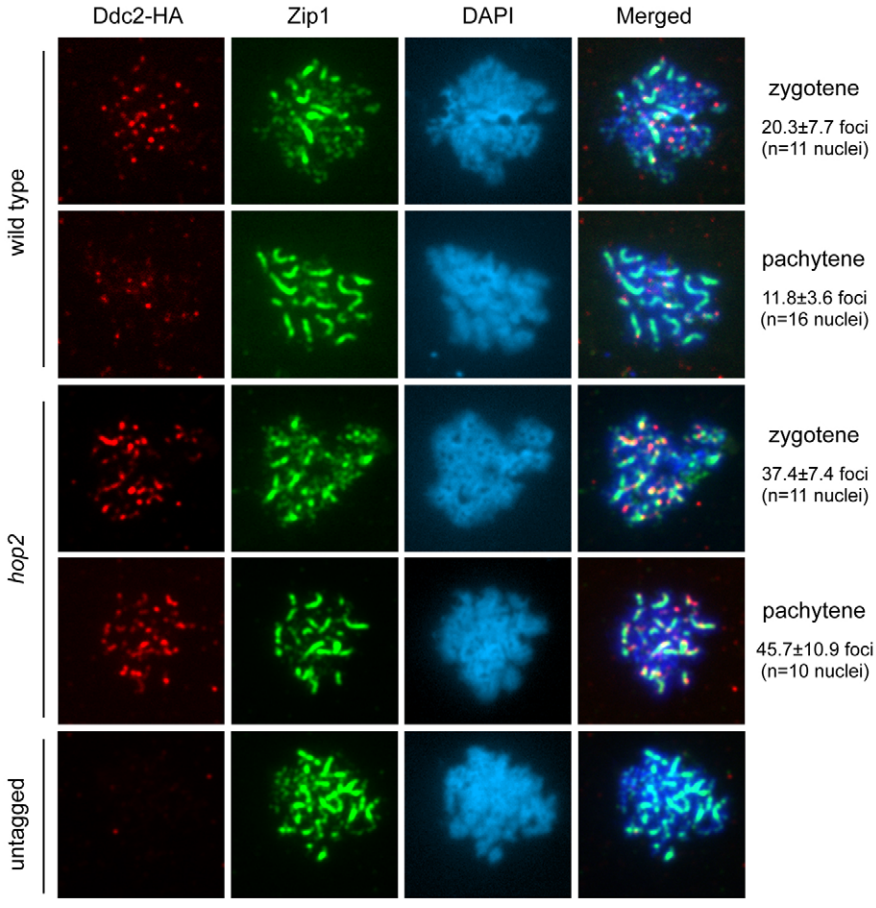

Fig. 4. Ddc2 localizes to meiotic chromosomes. Immunofluorescence of meiotic nuclear spreads stained with DAPI (blue), anti-HA (red) and anti-Zip1 (green) antibodies. Representative zygotene and pachytene nuclei, based on Zip1 staining, are shown. Quantification of the number of Ddc2 foci is presented to the right. Strains are DP487 (wild type), DP491 (*hop2*) and DP471 (untagged). Spreads were prepared 15 hours after meiotic induction.

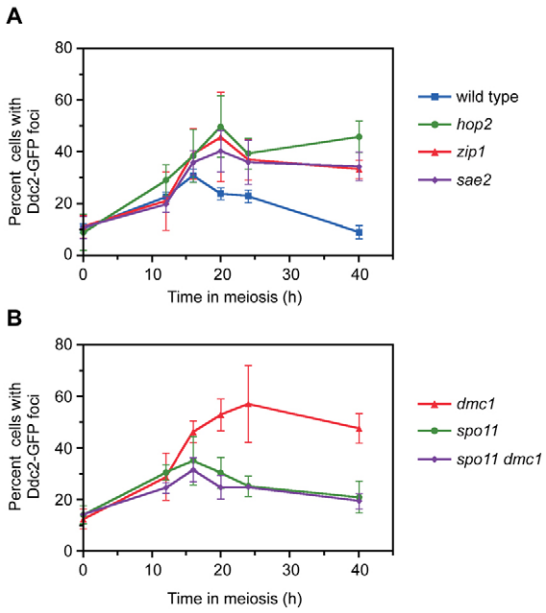

Fig. 5. Analysis of Ddc2–GFP localization in live meiotic cells. (**A**,**B**) The percentage of cells containing Ddc2–GFP signal at different times in meiosis is represented. Means + s.d. from two to six independent experiments are shown. Between 150 and 500 cells were scored for each strain at every time point in each experiment. Strains are DP448 (wild type), DP480 (*hop2*), DP449 (*zip1*), DP484 (*sae2*), DP450 (*dmc1*), DP465 (*spo11*) and DP469 (*spo11 dmc1*).

detected at single spots (Fig. 6). Moreover, the accumulation of cells displaying numerous Ddc2 foci at late time points that occurs in *dmc1* was suppressed in the *spo11 dmc1* double mutant (Fig. 5B, Fig. 6). Thus, these observations indicate that the pattern of Ddc2 localization in multiple contiguous foci is specific of meiotic DSBs engaged in the recombination process.

Recruitment of Ddc2 to DSBs in vegetative cells depends on the replication protein A (RPA) complex; therefore, we analyzed meiotic Ddc2-GFP foci formation in a hypomorphic *rfa1-t11* mutant, which retains the essential RPA function in DNA replication, but is deficient in its checkpoint function (Zou and Elledge, 2003). Interestingly, we found that the *dmc1 rfa1-t11* double mutant was severely impaired in Ddc2 foci formation during meiosis (Fig. 7A). Moreover, this reduced localization of Ddc2 to meiotic DSBs resulted in a defective checkpoint response because the *dmc1 rfa1-t11* double mutant showed impaired activation (phosphorylation) of the meiotic recombination checkpoint effector kinase Mek1 (Fig. 7B) and induction of the checkpoint target Cdc5 polo kinase (Fig. 7B), which marks exit from prophase, leading to a partial bypass of the *dmc1* meiotic delay (Fig. 7C). Thus, Ddc2 requires a functional RPA complex to properly perform its role in the meiotic recombination checkpoint.

Ddc2 accumulates at unrepaired meiotic DSBs

Meiotic localization studies of the Ddc2 protein, both on spread chromosomes and in live cells, are consistent with Ddc2 acting as a sensor of meiotic recombination intermediates. To confirm this, we analyzed by chromatin immunoprecipitation (ChIP) the binding of Ddc2 at two meiotic DSB hotspots (*BUD23* and *ERG1*) relative to the rDNA cold region where meiotic DSBs are absent. ChIP analysis was carried out in wild-type and *dmc1* cells before entering meiosis (t=0) and after 24 hours in meiosis, when Ddc2 foci accumulate in *dmc1* (see above; Fig. 5B, Fig. 6). In the wild type, no or little meiotic enrichment of Ddc2 was detected, which is consistent with DSBs being repaired. By contrast, a marked increment of Ddc2 was observed at both hotspots in *dmc1* cells after 24 hours in meiosis (Fig. 8A). Importantly, the enrichment was significantly decreased (P<0.01) in the absence of Spo11 (Fig. 8B), indicating that Ddc2 binds to sites of ongoing meiotic recombination.

Colocalization of ATRIP with ATR, TopBP1 and RPA in mouse meiotic chromosomes

To explore whether the meiotic localization of yeast Ddc2 is conserved through evolution, we studied the staining pattern of its mammalian homolog, ATRIP, on chromosome spreads of mouse spermatocytes. Co-staining of the SYCP3 component of the lateral elements of the SC was used to assess the meiotic stage of the nuclei on the spreads (Lammers et al., 1994). Interestingly, we found that during meiotic prophase I, ATRIP associated with the unsynapsed chromosome cores in zygotene spermatocytes as well as with SCs and the cores of the XY chromosome pair later in pachytene (Fig. 9A). As the SCs disassembled in diplotene, ATRIP displayed a more diffuse staining, but was still present on the sex body (Fig. 9A). In somatic cells, ATRIP together with TopBP1 are important for the ATR-dependent DNA damage response (Smits et al., 2010). Moreover, in previous studies of mice spermatocytes, we and others have demonstrated that the ATR and TopBP1 checkpoint proteins specifically localize to the unsynapsed regions of meiotic chromosomes (Keegan et al., 1996; Moens et al., 1999; Perera et al., 2004); therefore, we studied colocalization of ATRIP with ATR and TopBP1 during mammalian meiotic prophase. Interestingly, ATRIP extensively colocalized with ATR on the chromosome cores of the incompletely synapsed homologs, as well as on the cores and chromatin of the XY bivalent (Fig. 9B). A similar pattern was found for TopBP1, which displayed significant colocalization with ATRIP, mostly on unsynapsed autosomal regions and the XY pair (Fig. 9B; data not shown). Finally, we examined colocalization of ATRIP and the RPA complex, which is required for ATR/Mec1 signaling in both somatic mammalian cells and vegetative yeast cells (Zou and Elledge, 2003; Ball et al., 2005) and also associates to mouse meiotic chromosomes (Moens et al., 2002; Moens et al., 2007). Furthermore, RPA is required for efficient Ddc2 foci formation in DSB repair-deficient yeast meiotic cells (see above; Fig. 7). We found that RPA coexisted with ATRIP at both synapsed and unsynapsed chromosomal regions and showed a significant, although not absolute, colocalization (Fig. 9D). Strikingly, the colocalization of ATRIP and RPA diminished as synapsis progressed and the ATRIP signal became more continuous along the SCs. Thus, during some prophase stages in spermatocytes, ATRIP colocalizes with other proteins involved in several aspects of meiotic chromosome metabolism.

Discussion

Different meiotic mutants, such as *zip1*, *dmc1*, *hop2* or *sae2*, altered in various aspects of meiotic recombination and chromosome dynamics trigger checkpoint-mediated meiotic arrest or delay. To further understand meiotic checkpoint activation we have carried out a thorough functional characterization of the meiotic role of the Ddc2 checkpoint protein in yeast. In addition, we have examined the localization of the mammalian homolog, ATRIP, in mouse spermatocytes.

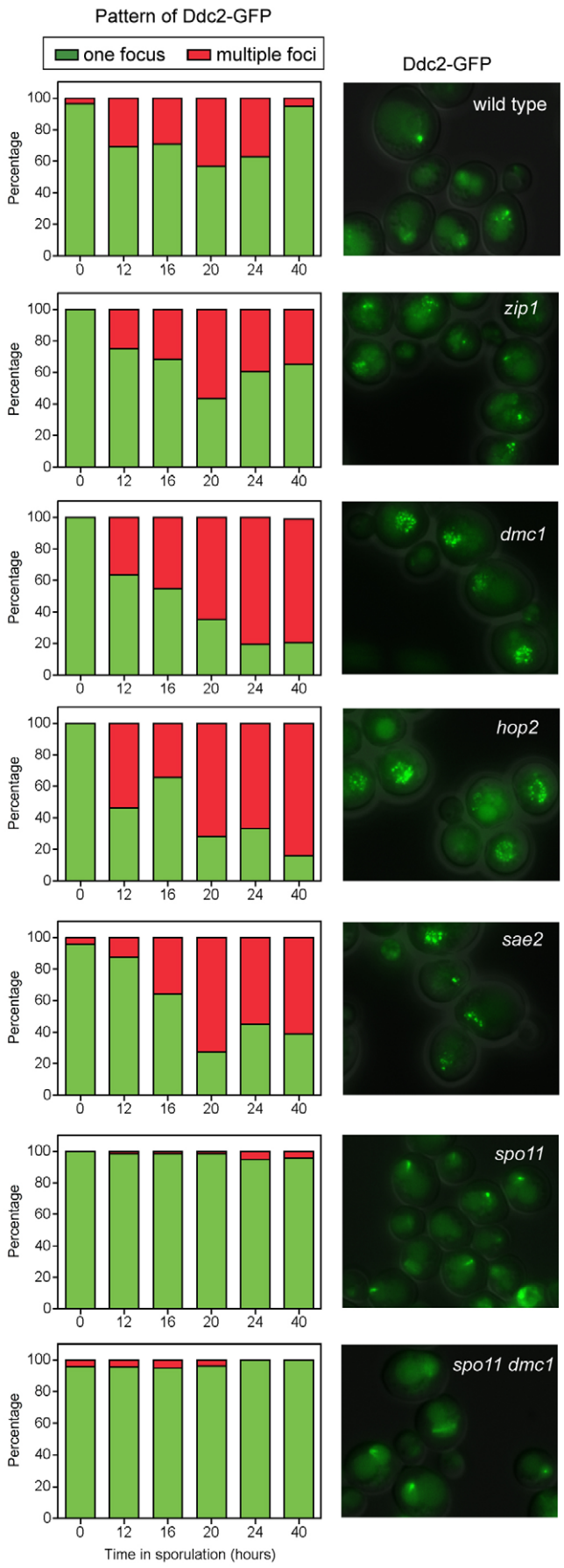

Meiotic checkpoint function of Ddc2

Deletion of *DDC2* suppresses the meiotic delay of all the mutants tested, implying that, together with Mec1 (Lydall et al., 1996; Usui et al., 2001), Ddc2 is a key regulator of meiotic surveillance mechanisms. The major chromosomal defect of the *zip1* mutant is the lack of synapsis, which results in homolog nondisjunction at meiosis I (Sym and Roeder, 1994) manifested by a characteristic pattern of spore death with a predominance of 4-, 2- and 0-spore-viable tetrads. However, in the *zip1 ddc2* double mutant the spore viability is further reduced and the pattern of *zip1* is lost (Fig. 1B), suggesting that cells enter meiosis with unresolved recombination intermediates. Nevertheless, like in *zip1*, most asci formed in *zip1 ddc2* are mature and spores contain intact nuclei, consistent with the fact that only a small fraction of DSBs remain unrepaired in the *zip1* mutant (Storlazzi et al., 1996; Xu et al., 1997).

In the BR strain background, the *dmc1* mutant exhibits a pronounced delay in meiosis, but eventually sporulates and produces some mature spores with intact nuclei. This observation suggests that, during the *dmc1* delay, a significant fraction of DSBs are repaired, probably using the sister chromatid as a template. Confirming this possibility, we observe that a *rad54 dmc1* double mutant displays a tighter arrest. Thus, the different meiotic progression phenotype of *dmc1* in SK1 (arrest) and BR (delay) strains might arise from a weaker barrier to sister chromatid recombination (Niu et al., 2009) in BR. In any case, deletion of *DDC2* bypasses the delay or arrest of both *dmc1* and *dmc1 rad54*, respectively, resulting in inviable spores with fragmented genetic material. The *hop2 ddc2* and *sae2 ddc2* mutants show the same type of aberrant meiotic products; i.e. inviable and immature spores with aberrant distribution of nuclear material. Although both *dmc1* and *hop2* are defective in DSB repair, the stronger meiotic block of *hop2* probably arises from the occurrence of non-homologous synapsis (Leu et al., 1998). The fact that, except for *zip1*, deletion of *DDC2* in *dmc1*, *hop2* or *sae2* does not result in wild-type kinetics of meiosis (as assessed by DAPI staining) probably stems from the difficulty in scoring meiotic divisions by DAPI when nuclei are fragmented as a consequence of chromosome segregation with unrepaired DSBs. In fact, analysis of spindle pole separation shows that the meiotic block of *dmc1* and *hop2* is completely bypassed by *DDC2* deletion (Fig. 2).

Regulation of Ddc2 during meiosis

We observed that Ddc2 protein levels peak at meiotic prophase coincident with the presence of recombination intermediates, but progressively decline as meiosis and sporulation progress. Interestingly, Ddc2 accumulates in checkpoint-arrested mutants, which is consistent with a role for Ddc2 in sensing meiotic recombination intermediates. DNA damage during the mitotic cell cycle stimulates the Mec1-dependent phosphorylation of Ddc2 in budding yeast, as well as ATR-dependent phosphorylation of ATRIP in mammalian cells (Paciotti et al., 2000; Itakura et al., 2004);

Fig. 6. Ddc2 localizes to multiple foci in mutants that accumulate meiotic recombination intermediates. The pattern of Ddc2–GFP localization throughout meiosis (one focus or multiple foci, as indicated) was scored among those cells containing Ddc2–GFP signal. The graphs (left panels) represent the percentage of each localization pattern. Representative images for each strain are also shown (right panels). Between 150 and 500 cells were scored for each strain at every time point. Strains used were the same as for Fig. 5.

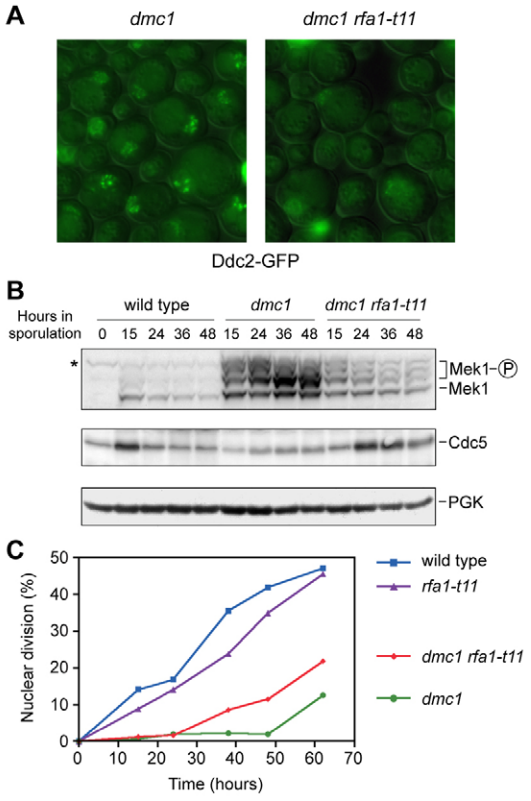

Fig. 7. Efficient meiotic Ddc2 foci formation is impaired in an RPA mutant (*rfa1-t11*) and results in a defective meiotic checkpoint response. (**A**) Representative images of Ddc2–GFP foci in *dmc1* and *dmc1 rfa1-t11* cells after 24 hours in meiosis. (**B**) Western blot analysis of Mek1 and Cdc5. PGK was used as a loading control. The Mek1 gel contained Phos-tag. The asterisk marks a nonspecific band. (**C**) Time course analysis of meiotic nuclear divisions. The percentage of cells containing more than two nuclei is represented. Strains are DP433 (wild type), DP506 (*rfa1-t11*), DP434 (*dmc1*) and DP505 (*dmc1 rfa1-t11*).

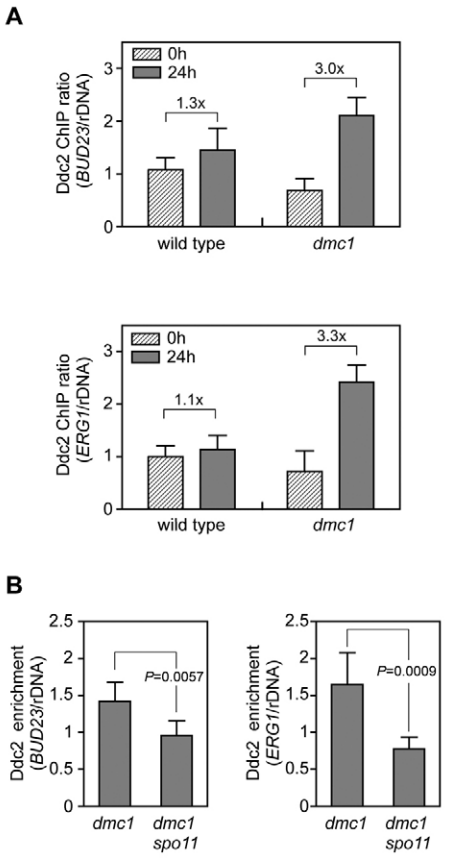

Fig. 8. Ddc2 binds to sites of meiotic recombination sensing unrepaired DSBs. (**A**) ChIP analysis of Ddc2 recruitment to the *BUD23* and *ERG1* DSB hotspots in wild-type (DP487) and *dmc1* (DP488) strains carrying *DDC2-HA*, using anti-HA antibodies. Input and immunoprecipitated DNA from samples taken at 0 hours and 24 hours in meiosis were analyzed by quantitative real-time PCR using primer pairs located at the hotspot positions, and at the rDNA as a control for a chromosomal region with no meiotic DSBs. Ddc2 enrichment at each hotspot, normalized to the rDNA, is represented. The mean fold-increase of Ddc2 recruitment during meiosis (t=24 hours) relative to vegetative cells (t=0 hours) is indicated above the bars. Means + s.d. from three independent experiments are shown. (**B**) ChIP analysis of Ddc2–HA recruitment to the *BUD23* and *ERG1* hotspots relative to the rDNA cold region in *dmc1* (DP693) and *dmc1 spo11* (DP695) cells at 24 hours in meiosis. Note that the strains are also *ndt80* to arrest meiotic progression in prophase. Means + s.d. and P-values for six independent experiments are shown.

however, the contribution of these phosphorylation events to damage signaling remains largely elusive (Zou, 2007). Strikingly, we found that mutation of the three consensus [S/T]Q sites for Mec1 phosphorylation present in Ddc2 do not confer any checkpoint defect either in mitotic or meiotic cells, indicating that these potential phosphorylation sites are not relevant for the checkpoint function of Ddc2. Similarly, in somatic mammalian cells, ATR-dependent phosphorylation of ATRIP at [S/T]Q sites is dispensable for the DNA damage response (Itakura et al., 2004). The lack of biological relevance for [S/T]Q phosphorylation sites in other Mec1 targets, such as Xrs2, Dun1 and Rfa2, has also been reported (Mallory et al., 2003). Perhaps, more sensitive assays are required to reveal a functional importance for those sites in some Mec1/ATR substrates.

Ddc2 signals meiotic recombination intermediates

In vegetative cells, the Mec1–Ddc2 complex is a primary sensor of DNA damage (Kondo et al., 2001; Melo et al., 2001) and formation of Ddc2 foci has been widely used as a marker for the presence of DNA damage (Lisby et al., 2004). Although Mec1–Ddc2 might recognize different types of aberrant or damaged DNA structures, at least it has been unequivocally determined that single-stranded DNA (ssDNA) coated by RPA is bound by the Mec1–Ddc2 complex (Zou and Elledge, 2003; Nakada et al., 2005; Zou, 2007). Here, we provide evidence indicating that Ddc2 also senses the presence of recombination intermediates during meiosis. Ddc2 localization to meiotic chromosomes correlates with the dynamics of DSB repair during meiotic prophase; Ddc2 foci are abundant in zygotene but diminish by pachytene in wild-type cells. By contrast, the number of Ddc2 foci remains elevated in *dmc1* and *hop2* mutants that accumulate unrepaired DSBs. The fact that the number of meiotic Ddc2 foci observed on chromosome spreads (~30–60) is lower than the total number of meiotic DSBs (~200) might reflect the fact that a single focus represents several unrepaired DSBs. Interestingly, the number of foci and timing of distribution on meiotic chromosomes of the Ddc1 checkpoint protein is similar

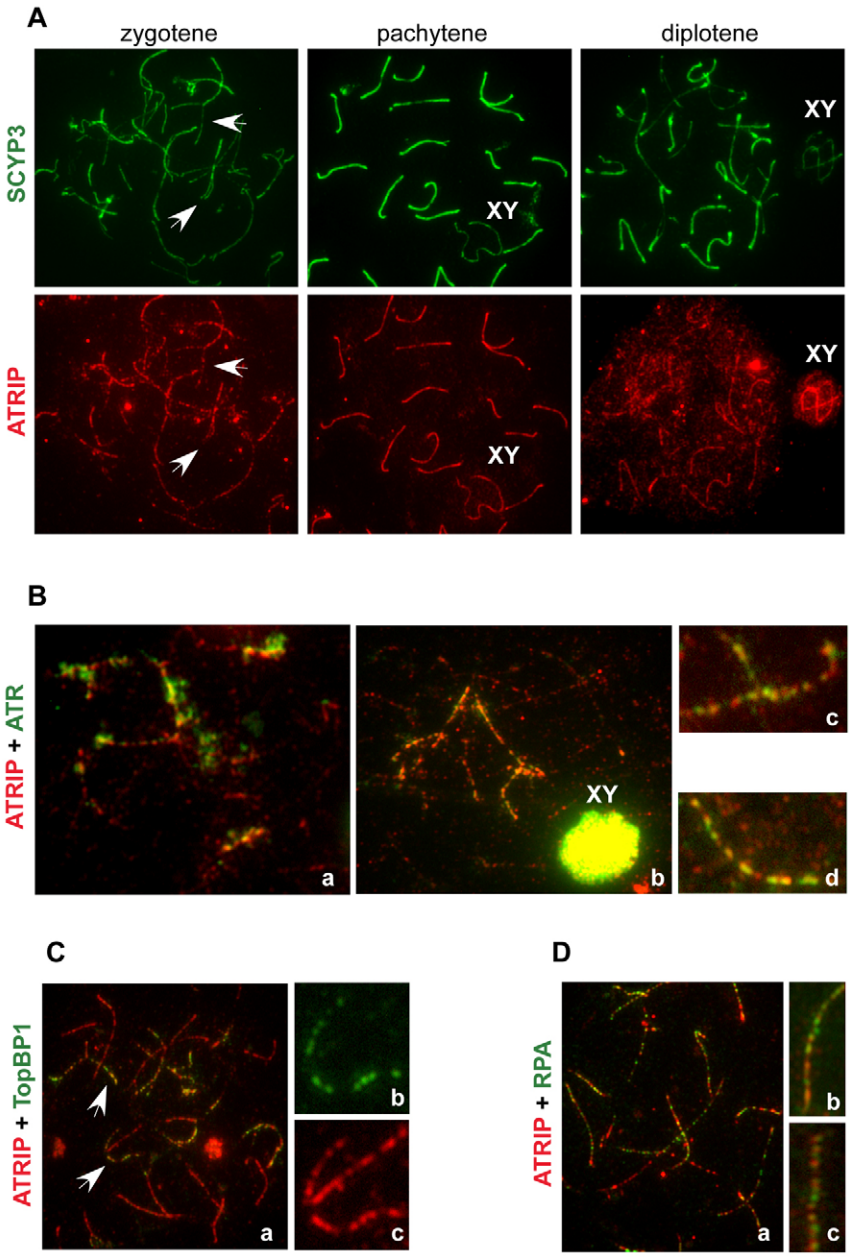

Fig. 9. ATRIP colocalizes with ATR, TopBP1 and RPA on mouse meiotic chromosomes. (**A**) ATRIP associates with chromosome cores from zygotene to early diplotene. Representative images of chromosome spreads from mouse spermatocytes of the indicated meiotic prophase stages are shown, stained with anti-SCYP3 (green) and anti-ATRIP (red) antibodies. Arrows point to unsynapsed autosomal regions. (**B**) Colocalization of ATR and ATRIP on unsynapsed bivalents. Merged images of two nuclei (Ba,Bb) stained with anti-ATR (green) and anti-ATRIP (red); overlap appears yellow. Bc and Bd show close-ups of bivalents. (**C**) Colocalization of TopBP1 and ATRIP on unsynapsed autosomal regions (arrows). Merged image of a late zygotene nucleus (Ca) stained with anti-TopBP1 (green) and anti-ATRIP (red) antibodies; overlap appears yellow. Cb and Cc show close-up views of a partially synapsed bivalent to exhibit the TopBP1 and ATRIP colocalization in the unsynapsed portion. (**D**) RPA (green) and ATRIP (red) localize to the SC. Da shows a representative merged image. Note that there are regions where RPA is lost, but ATRIP persists. Db and Dc, show a close-up views of bivalents to exhibit the high degree of ATRIP and RPA colocalization. XY, sex body.

to that of Ddc2 (Hong and Roeder, 2002), despite their independent recruitment to DSBs (Melo et al., 2001).

In vegetative cells, the presence of DSBs induces the formation of the 'repair centers' in which a number of DNA repair and checkpoint proteins, including Ddc2, can be visualized as discrete nuclear foci in whole cells (Lisby et al., 2004). It has been shown that each focus represents multiple DSBs (Lisby et al., 2003b) and although they are induced by DNA damage, the repair foci also appear in undamaged cells and probably represent spontaneous damage generated during DNA replication (Lisby et al., 2003a). Our time-course analysis of Ddc2–GFP foci in live meiotic cells is also consistent with a role for Ddc2 in signaling meiotic recombination intermediates. In the wild type, cells containing Ddc2 foci reach a maximum during meiotic prophase and then decrease, whereas in recombination-defective mutants Ddc2-positive cells accumulate.

It is also noteworthy to mention the different morphology of Ddc2–GFP foci in mitotic versus meiotic live cells. In mitotic cells, multiple DSBs result in only one or very few centers visualized as prominent foci where checkpoint and DNA repair proteins are brought together. This reduced number of foci (1–3) arises even from high γ-radiation doses producing about 80 DSBs per cell (Lisby et al., 2003b). By contrast, in meiotic cells we observe numerous Ddc2 foci coincident with the presence of unrepaired DSBs. This different pattern might reflect not only the great number of meiotic DSBs generated in a single cell, but also the specialized chromosomal architecture in which meiotic DSB formation, signaling and repair occur. Moreover, we observed different morphologies for Ddc2 foci among the meiotic mutants analyzed: the *sae2* mutant displays fewer and brighter Ddc2–GFP foci than *hop2* or *dmc1*, probably manifesting the different stage in which DSB repair is blocked. The formation of Ddc2 foci in

sae2 cells was somehow surprising because Sae2 is required for DSBs resection. This observation implies that, at least in BR strains, some ssDNA must be formed under these circumstances. Future investigations will shed light into this unexpected finding.

Ddc2 meiotic foci formation depends on Spo11, i.e. in initiation of meiotic recombination, and partially colocalize with Rad51 indicating that they represent bona fide sites of ongoing meiotic recombination. A limited colocalization of Rad51 and Dmc1 foci with the ATR or TopBP1 checkpoint proteins has been also reported on mammalian meiotic chromosomes (Moens et al., 1999; Perera et al., 2004). The fact that we observed only a partial colocalization of Ddc2 and Rad51 on meiotic chromosome spreads suggests that their recruitment to recombination intermediates might occur with different timing. Consistent with this possibility, molecular and biochemical analyses of recombinational DSB repair have demonstrated that, during strand invasion, Rad51 displaces RPA from ssDNA (Kantake et al., 2003; Sugiyama and Kantake, 2009). If Ddc2 preferentially binds to RPA-coated sites, as suggested by the impaired formation of meiotic Ddc2 foci in RPA-deficient cells (Fig. 7), this might explain the lack of complete colocalization between Ddc2 and Rad51, as also described for Ddc1 and Rad51 (Hong and Roeder, 2002). The marked variability in the relative intensity of Ddc2 and Rad51 foci is also consistent with different dynamics of chromosomal localization of the two proteins. In any case, ChIP analysis of a *dmc1* mutant reveals a Spo11-dependent meiosis-specific accumulation of Ddc2 at two DSB hotspots, which corroborates the presence of Ddc2 at meiotic recombination intermediates. The modest, though significant, enrichment of Ddc2 at the DSB sites analyzed might reflect a milder hotspot activity in BR strains.

Evolutionary conservation of Ddc2/ATRIP meiotic function

To gain insight into the possible conservation of the Ddc2 meiotic function through evolution we have also carried out a cytological analysis of mammalian ATRIP during male mouse gametogenesis. Although protein localization studies can only provide tentative conclusions regarding biological relevance, cytological studies of mammalian meiosis, where functional analyses are often technically problematic, have proven to be highly productive in revealing important features of various meiotic events (Page et al., 1998; Moens et al., 2002; Marcon and Moens, 2003; Parra et al., 2004; Viera et al., 2007; Parra et al., 2009). We find that ATRIP localizes to mouse meiotic chromosomes during the leptotene to pachytene stages of meiotic prophase. However, at diplotene the majority of ATRIP is found on the sex body, where the XY pair remains unsynapsed and virtually all checkpoint proteins analyzed are detected (Keegan et al., 1996; Freire et al., 1998; Moens et al., 1999; Perera et al., 2004; Lee et al., 2005; Roig et al., 2010). We also find extensive colocalization of ATRIP with ATR and TopBP1, particularly on autosomal regions that remain unsynapsed. It has been proposed that the presence of ATR and TopBP1 at those regions is a manifestation of their role in monitoring meiotic recombination and signaling the existence of recombination intermediates to activate the pachytene checkpoint (Perera et al., 2004). The presence of ATRIP at the same locations is also consistent with such a role, as we have demonstrated for yeast Ddc2. Remarkably, ATRIP also remains on the synapsed chromosomes when the bulk of ATR, TopBP1 and, to some extent, RPA have disappeared, raising the possibility of an additional function for ATRIP in meiotic chromosome dynamics (Marcon and Moens, 2005). Future studies aimed to the identification of novel meiotic interacting partners of ATRIP might shed light into this possibility.

In summary, our cytological analysis of ATRIP in mammalian germ cells is consistent with a functional role for ATRIP in mammalian meiosis similar, at least is some aspects, to the meiotic function of the yeast homolog Ddc2 described in this study as a sensor of meiotic recombination intermediates. Thus, our results hint at an evolutionary conservation for the biological significance of Ddc2/ATRIP in the specialized meiotic cell cycle.

Materials and Methods

Yeast strains and plasmids

Yeast strains genotypes are listed in supplementary material Table S1. All the strains are in the BR1919 background (Rockmill and Roeder, 1990), except those used in Fig. 7, which are in the W303 background. The *DDC2-GFP::TRP1* and *DDC2-3HA::kanMX6* tagging, as well as the *ddc2::TRP1*, *sml1::kanMX6*, *dmc1::kanMX6*, *dmc1::hphMX4* and *sae2::kanMX6* gene deletions were performed using PCR-based approaches (Longtine et al., 1998; Goldstein and McCusker, 1999). To generate *TUB1-GFP::TRP1* strains, the *Hin*dIII-cut plasmid B237 (a gift from Beth Rockmill, Yale University, New Haven, CT) was used. The *zip1::LYS2*, *spo11::ADE2*, *hop2::LEU2* and *rad54::LEU2* gene disruptions have been previously described (Leu et al., 1998; San-Segundo and Roeder, 1999; San-Segundo and Roeder, 2000). All strains were constructed either by direct transformation or by genetic crosses always in an isogenic background. Strains harboring the *rfa1-t11* allele derived from CY5467 (Lucca et al., 2004). Plasmid pSS136, containing *ddc2-3AQ-myc*, was constructed by site-directed mutagenesis of pLCD1-myc, which expresses *myc*-tagged *DDC2* under its own promoter (Rouse and Jackson, 2002), using the QuickChange kit (Stratagene). For meiotic time courses, strains were grown in 2×SC (3.5 ml) for 20–24 hours, then transferred to YPDA (2.5 ml) and incubated to saturation for an additional 8 hours. Cells were harvested, washed with 2% potassium acetate (KAc), resuspended into 2% KAc (10 ml) and incubated at 30°C with vigorous shaking to induce meiosis and sporulation. Both YPDA and 2% KAc were supplemented with 20 mM adenine and 10 mM uracil. The culture volumes were scaled-up when needed.

Western blotting

TCA cell extracts from 5–10 ml aliquots of meiotic cultures were prepared and analyzed as described (Conde and San-Segundo, 2008). In-house produced mouse monoclonal anti-HA and rabbit polyclonal anti-GFP were used at 1:2000 dilution. Mouse monoclonal anti-myc (9E10, Covance) and goat polyclonal anti-Rad53 (sc-6749) and anti-Cdc5 (sc-6733), from Santa Cruz Biotechnology, were used at 1:1000 dilution. Anti-PGK monoclonal antibody 22C5 (A-6457, Molecular Probes) was used at 1:5000. The rabbit polyclonal Mek1 antibody (used at 1:1000 dilution) was raised against a recombinant His6-tagged full-length Mek1 protein expressed in *Escherichia coli*. To resolve the phosphorylated forms of Mek1, 10% SDS-PAGE gels containing 37.5 μM Phos-tag reagent (NARD Institute, Amagasaki City, Japan) were used. The ECL or ECL+ reagents (GE Healthcare) were used for detection and the Quantity One software (Bio-Rad) to quantify protein levels.

Yeast cytology

Immunofluorescence of chromosome spreads was performed as described (San-Segundo and Roeder, 1999). To detect Ddc2–HA or Ddc2–GFP, the mouse monoclonal anti-HA (HA.11, Covance) or the rabbit polyclonal anti-GFP antibodies, respectively, were used at 1:200 dilution. Mouse anti-tubulin antibody (TAT1, a gift from Keith Gull, University of Oxford, UK) was used at 1:500. Rabbit anti-Rad51 (a gift from Douglas Bishop, University of Chicago, Chicago, IL) and anti-Zip1 (a gift from G. Shirleen Roeder, Yale University, New Haven, CT) antibodies were used at 1:750 and 1:100 dilutions, respectively. Alexa-Fluor-488- and Alex-Fluor-594-conjugated secondary antibodies from Molecular Probes were used at 1:200 dilution.

Images were captured with a Nikon Eclipse 90i fluorescence microscope controlled with the MetaMorph software (Molecular Devices, Silicon Valley, CA) and equipped with an Orca-AG (Hamamatsu) CCD camera and a PlanApo VC 100× 1.4 NA objective. To analyze Ddc2–GFP foci in live meiotic cells, for each field, 11 Z-planes at 0.4 μm intervals were captured with 1 second of exposure time and processed with NIH ImageJ software (http://rsb.info.nih.gov/ij/). Maximum-intensity projections of the planes containing the signal are presented.

Mouse cytology

Spreading and immunostaining of mouse testicular preparations were performed as previously reported (Perera et al., 2004). The rabbit polyclonal ATRIP antibody was raised against a recombinant fragment of His-tagged human ATRIP comprising amino acid residues 10–120 purified from *E. coli*. Antibodies to SYCP3 (Dobson et al., 1994), ATR (Perera et al., 2004), TopBP1 (Perera et al., 2004) and RPA (Kolas et al., 2005) have been described.

Chromatin immunoprecipitation

Aliquots of cells (8 ml) at *t*=0 hours or *t*=24 hours in meiosis were fixed with 1% formaldehyde for 10–15 minutes, treated with 125 mM glycine for 5 minutes, washed with ice-cold PBS and stored at –80°C until processing. ChIP was performed essentially as described (Buhler et al., 2009) with the following modifications. Chromatin was fragmented using a Bioruptor (Diagenode, Liège, Belgium) by three cycles of sonication during 10 minutes in iced-water with pulses of 30 seconds 'on' and 60 seconds 'off'. Additional washing steps of the immunoprecipitates were performed and the DNA purified using Chelex 100 (Bio-Rad) (Nelson et al., 2006). DNA was analyzed by quantitative PCR in an ABI7000 machine (Applied Biosystems) using previously described primer pairs for the *BUD23* and *ERG1* DSB hotspots, as well as for the rDNA as a control for no DSBs, which was used for normalization (Buhler et al., 2009). Each sample of input and immunoprecipitated (IP) DNA was analyzed in triplicate in every experiment. Each experiment was repeated three to six times, as indicated. Enrichment of Ddc2–HA at the meiotic hotspots was calculated as follows: $(IP^{hotspot}/INPUT^{hotspot})/(IP^{rDNA}/INPUT^{rDNA})$.

Other techniques

To analyze meiotic nuclear divisions, cells were fixed in 70% ethanol, washed in PBS and stained with 1 μg/μl DAPI for 15 minutes at room temperature. Dityrosine fluorescence (San-Segundo and Roeder, 2000) and DNA damage sensitivity assays (Conde and San-Segundo, 2008) have been previously described. To calculate the statistical significance of differences, a two-tailed Student *t*-test was used. *P*-values were calculated using the GraphPad Prism 4.0 software. $P<0.01$ was considered significant.

We thank Douglas Bishop, Steve Jackson, Félix Prado, Beth Rockmill, Shirleen Roeder, John Rouse and José A. Tercero for providing reagents. We acknowledge Peter Moens, who contributed to ATRIP characterization, but passed away before this manuscript could be published. We are grateful to Félix Prado and José Pérez-Martín for comments, to Alfredo Santana for preliminary work on ATRIP, to Michael Lichten for advice on ChIP, to David Ontoso for advice on Mek1 phosphorylation analysis and to other P.S.-S. laboratory members for suggestions. E.R. was supported by a predoctoral fellowship from the Ministry of Science and Innovation of Spain (MICINN) and S.C. by a JAE-Doc contract from CSIC (Spain). Research in our laboratories is funded by grants from MICINN (SAF2007-64361 and CSD2007-00015 to R.F. and BFU2009-07159 to P.S.-S.), FUNCIS (PI27/062) to R.F., and Fundación Ramón Areces to P.S.-S.

Supplementary material available online at
http://jcs.biologists.org/cgi/content/full/124/14/2488/DC1

References

Arbel, A., Zenvirth, D. and Simchen, G. (1999). Sister chromatid-based DNA repair is mediated by *RAD54*, not by *DMC1* or *TID1*. *EMBO J.* **18**, 2648-2658.

Bailis, J. M., Smith, A. V. and Roeder, G. S. (2000). Bypass of a meiotic checkpoint by overproduction of meiotic chromosomal proteins. *Mol. Cell. Biol.* **20**, 4838-4848.

Ball, H. L., Myers, J. S. and Cortez, D. (2005). ATRIP binding to replication protein A-single-stranded DNA promotes ATR-ATRIP localization but is dispensable for Chk1 phosphorylation. *Mol. Biol. Cell* **16**, 2372-2381.

Barchi, M., Mahadevaiah, S., Di Giacomo, M., Baudat, F., de Rooij, D. G., Burgoyne, P. S., Jasin, M. and Keeney, S. (2005). Surveillance of different recombination defects in mouse spermatocytes yields distinct responses despite elimination at an identical developmental stage. *Mol. Cell. Biol.* **25**, 7203-7215.

Bhalla, N. and Dernburg, A. F. (2005). A conserved checkpoint monitors meiotic chromosome synapsis in *Caenorhabditis elegans*. *Science* **310**, 1683-1686.

Bishop, D. K., Park, D., Xu, L. and Kleckner, N. (1992). *DMC1*: a meiosis-specific yeast homolog of E. coli *recA* required for recombination, synaptonemal complex formation, and cell cycle progression. *Cell* **69**, 439-456.

Borner, G. V. (2006). Balancing the checks: surveillance of chromosomal exchange during meiosis. *Biochem. Soc. Trans.* **34**, 554-556.

Borner, G. V., Kleckner, N. and Hunter, N. (2004). Crossover/noncrossover differentiation, synaptonemal complex formation, and regulatory surveillance at the leptotene/zygotene transition of meiosis. *Cell* **117**, 29-45.

Buhler, C., Shroff, R. and Lichten, M. (2009). Genome-wide mapping of meiotic DNA double-strand breaks in *Saccharomyces cerevisiae*. *Methods Mol. Biol.* **557**, 143-164.

Carballo, J. A., Johnson, A. L., Sedgwick, S. G. and Cha, R. S. (2008). Phosphorylation of the axial element protein Hop1 by Mec1/Tel1 ensures meiotic interhomolog recombination. *Cell* **132**, 758-770.

Chen, Y. K., Leng, C. H., Olivares, H., Lee, M. H., Chang, Y. C., Kung, W. M., Ti, S. C., Lo, Y. H., Wang, A. H., Chang, C. S. et al. (2004). Heterodimeric complexes of Hop2 and Mnd1 function with Dmc1 to promote meiotic homolog juxtaposition and strand assimilation. *Proc. Natl. Acad. Sci. USA* **101**, 10572-10577.

Chu, S. and Herskowitz, I. (1998). Gametogenesis in yeast is regulated by a transcriptional cascade dependent on Ndt80. *Mol. Cell* **1**, 685-696.

Conde, F. and San-Segundo, P. A. (2008). Role of Dot1 in the response to alkylating DNA damage in *Saccharomyces cerevisiae*: regulation of DNA damage tolerance by the error-prone polymerases Polζ/Rev1. *Genetics* **179**, 1197-1210.

de Rooij, D. G. and de Boer, P. (2003). Specific arrests of spermatogenesis in genetically modified and mutant mice. *Cytogenet. Genome Res.* **103**, 267-276.

Dobson, M. J., Pearlman, R. E., Karaiskakis, A., Spyropoulos, B. and Moens, P. B. (1994). Synaptonemal complex proteins: occurrence, epitope mapping and chromosome disjunction. *J. Cell Sci.* **107**, 2749-2760.

Eichinger, C. S. and Jentsch, S. (2010). Synaptonemal complex formation and meiotic checkpoint signaling are linked to the lateral element protein Red1. *Proc. Natl. Acad. Sci. USA* **107**, 11370-11375.

Freire, R., Murguia, J. R., Tarsounas, M., Lowndes, N. F., Moens, P. B. and Jackson, S. P. (1998). Human and mouse homologs of *Schizosaccharomyces pombe rad1(+)* and *Saccharomyces cerevisiae RAD17*: linkage to checkpoint control and mammalian meiosis. *Genes Dev.* **12**, 2560-2573.

Gasior, S. L., Wong, A. K., Kora, Y., Shinohara, A. and Bishop, D. K. (1998). Rad52 associates with RPA and functions with Rad55 and Rad57 to assemble meiotic recombination complexes. *Genes Dev.* **12**, 2208-2221.

Goldstein, A. L. and McCusker, J. H. (1999). Three new dominant drug resistance cassettes for gene disruption in *Saccharomyces cerevisiae*. *Yeast* **15**, 1541-1553.

Harrison, J. C. and Haber, J. E. (2006). Surviving the breakup: the DNA damage checkpoint. *Annu. Rev. Genet.* **40**, 209-235.

Hassold, T. and Hunt, P. (2001). To err (meiotically) is human: the genesis of human aneuploidy. *Nat. Rev. Genet.* **2**, 280-291.

Henry, J. M., Camahort, R., Rice, D. A., Florens, L., Swanson, S. K., Washburn, M. P. and Gerton, J. L. (2006). Mnd1/Hop2 facilitates Dmc1-dependent interhomolog crossover formation in meiosis of budding yeast. *Mol. Cell. Biol.* **26**, 2913-2923.

Hochwagen, A. and Amon, A. (2006). Checking your breaks: surveillance mechanisms of meiotic recombination. *Curr. Biol.* **16**, R217-R228.

Hochwagen, A., Tham, W. H., Brar, G. A. and Amon, A. (2005). The FK506 binding protein Fpr3 counteracts protein phosphatase 1 to maintain meiotic recombination checkpoint activity. *Cell* **122**, 861-873.

Hong, E. J. and Roeder, G. S. (2002). A role for Ddc1 in signaling meiotic double-strand breaks at the pachytene checkpoint. *Genes Dev.* **16**, 363-376.

Itakura, E., Umeda, K., Sekoguchi, E., Takata, H., Ohsumi, M. and Matsuura, A. (2004). ATR-dependent phosphorylation of ATRIP in response to genotoxic stress. *Biochem. Biophys. Res. Commun.* **323**, 1197-1202.

Joyce, E. F. and McKim, K. S. (2009). Drosophila PCH2 is required for a pachytene checkpoint that monitors double-strand-break-independent events leading to meiotic crossover formation. *Genetics* **181**, 39-51.

Kantake, N., Sugiyama, T., Kolodner, R. D. and Kowalczykowski, S. C. (2003). The recombination-deficient mutant RPA (*rfa1-t11*) is displaced slowly from single-stranded DNA by Rad51 protein. *J. Biol. Chem.* **278**, 23410-23417.

Keegan, K. S., Holtzman, D. A., Plug, A. W., Christenson, E. R., Brainerd, E. E., Flaggs, G., Bentley, N. J., Taylor, E. M., Meyn, M. S., Moss, S. B. et al. (1996). The Atr and Atm protein kinases associate with different sites along meiotically pairing chromosomes. *Genes Dev.* **10**, 2423-2437.

Keeney, S., Giroux, C. N. and Kleckner, N. (1997). Meiosis-specific DNA double-strand breaks are catalyzed by Spo11, a member of a widely conserved protein family. *Cell* **88**, 375-384.

Kolas, N. K., Svetlanov, A., Lenzi, M. L., Macaluso, F. P., Lipkin, S. M., Liskay, R. M., Greally, J., Edelmann, W. and Cohen, P. E. (2005). Localization of MMR proteins on meiotic chromosomes in mice indicates distinct functions during prophase I. *J. Cell Biol.* **171**, 447-458.

Kondo, T., Wakayama, T., Naiki, T., Matsumoto, K. and Sugimoto, K. (2001). Recruitment of Mec1 and Ddc1 checkpoint proteins to double-strand breaks through distinct mechanisms. *Science* **294**, 867-870.

Lammers, J. H., Offenberg, H. H., van Aalderen, M., Vink, A. C., Dietrich, A. J. and Heyting, C. (1994). The gene encoding a major component of the lateral elements of synaptonemal complexes of the rat is related to X-linked lymphocyte-regulated genes. *Mol. Cell. Biol.* **14**, 1137-1146.

Lee, A. C., Fernandez-Capetillo, O., Pisupati, V., Jackson, S. P. and Nussenzweig, A. (2005). Specific association of mouse MDC1/NFBD1 with NBS1 at sites of DNA-damage. *Cell Cycle* **4**, 177-182.

Leu, J. Y. and Roeder, G. S. (1999). The pachytene checkpoint in *S. cerevisiae* depends on Swe1-mediated phosphorylation of the cyclin-dependent kinase Cdc28. *Mol. Cell* **4**, 805-814.

Leu, J. Y., Chua, P. R. and Roeder, G. S. (1998). The meiosis-specific Hop2 protein of *S. cerevisiae* ensures synapsis between homologous chromosomes. *Cell* **94**, 375-386.

Lisby, M., Antunez de Mayolo, A., Mortensen, U. H. and Rothstein, R. (2003a). Cell cycle-regulated centers of DNA double-strand break repair. *Cell Cycle* **2**, 479-483.

Lisby, M., Mortensen, U. H. and Rothstein, R. (2003b). Colocalization of multiple DNA double-strand breaks at a single Rad52 repair centre. *Nat. Cell Biol.* **5**, 572-577.

Lisby, M., Barlow, J. H., Burgess, R. C. and Rothstein, R. (2004). Choreography of the DNA damage response: spatiotemporal relationships among checkpoint and repair proteins. *Cell* **118**, 699-713.

Longhese, M. P., Bonetti, D., Guerini, I., Manfrini, N. and Clerici, M. (2009). DNA double-strand breaks in meiosis: checking their formation, processing and repair. *DNA Repair* **8**, 1127-1138.

Longtine, M. S., McKenzie, A., 3rd, Demarini, D. J., Shah, N. G., Wach, A., Brachat, A., Philippsen, P. and Pringle, J. R. (1998). Additional modules for versatile and economical PCR-based gene deletion and modification in *Saccharomyces cerevisiae*. *Yeast* **14**, 953-961.

Lucca, C., Vanoli, F., Cotta-Ramusino, C., Pellicioli, A., Liberi, G., Haber, J. and Foiani, M. (2004). Checkpoint-mediated control of replisome-fork association and signalling in response to replication pausing. *Oncogene* **23**, 1206-1213.
Lydall, D., Nikolsky, Y., Bishop, D. K. and Weinert, T. (1996). A meiotic recombination checkpoint controlled by mitotic checkpoint genes. *Nature* **383**, 840-843.
Mallory, J. C., Bashkirov, V. I., Trujillo, K. M., Solinger, J. A., Dominska, M., Sung, P., Heyer, W. D. and Petes, T. D. (2003). Amino acid changes in Xrs2p, Dun1p, and Rfa2p that remove the preferred targets of the ATM family of protein kinases do not affect DNA repair or telomere length in *Saccharomyces cerevisiae*. *DNA Repair* **2**, 1041-1064.
Marcon, E. and Moens, P. (2003). MLH1p and MLH3p localize to precociously induced chiasmata of okadaic-acid-treated mouse spermatocytes. *Genetics* **165**, 2283-2287.
Marcon, E. and Moens, P. B. (2005). The evolution of meiosis: recruitment and modification of somatic DNA-repair proteins. *BioEssays* **27**, 795-808.
McKee, A. H. and Kleckner, N. (1997). A general method for identifying recessive diploid-specific mutations in *Saccharomyces cerevisiae*, its application to the isolation of mutants blocked at intermediate stages of meiotic prophase and characterization of a new gene *SAE2*. *Genetics* **146**, 797-816.
Melo, J. A., Cohen, J. and Toczyski, D. P. (2001). Two checkpoint complexes are independently recruited to sites of DNA damage in vivo. *Genes Dev.* **15**, 2809-2821.
Moens, P. B., Tarsounas, M., Morita, T., Habu, T., Rottinghaus, S. T., Freire, R., Jackson, S. P., Barlow, C. and Wynshaw-Boris, A. (1999). The association of ATR protein with mouse meiotic chromosome cores. *Chromosoma* **108**, 95-102.
Moens, P. B., Kolas, N. K., Tarsounas, M., Marcon, E., Cohen, P. E. and Spyropoulos, B. (2002). The time course and chromosomal localization of recombination-related proteins at meiosis in the mouse are compatible with models that can resolve the early DNA-DNA interactions without reciprocal recombination. *J. Cell Sci.* **115**, 1611-1622.
Moens, P. B., Marcon, E., Shore, J. S., Kochakpour, N. and Spyropoulos, B. (2007). Initiation and resolution of interhomolog connections: crossover and non-crossover sites along mouse synaptonemal complexes. *J. Cell Sci.* **120**, 1017-1027.
Nakada, D., Hirano, Y., Tanaka, Y. and Sugimoto, K. (2005). Role of the C terminus of Mec1 checkpoint kinase in its localization to sites of DNA damage. *Mol. Biol. Cell* **16**, 5227-5235.
Nelson, J. D., Denisenko, O. and Bomsztyk, K. (2006). Protocol for the fast chromatin immunoprecipitation (ChIP) method. *Nat. Protoc.* **1**, 179-185.
Niu, H., Wan, L., Busygina, V., Kwon, Y., Allen, J. A., Li, X., Kunz, R. C., Kubota, K., Wang, B., Sung, P. et al. (2009). Regulation of meiotic recombination via Mek1-mediated Rad54 phosphorylation. *Mol. Cell* **36**, 393-404.
Paciotti, V., Clerici, M., Lucchini, G. and Longhese, M. P. (2000). The checkpoint protein Ddc2, functionally related to *S. pombe* Rad26, interacts with Mec1 and is regulated by Mec1-dependent phosphorylation in budding yeast. *Genes Dev.* **14**, 2046-2059.
Page, J., Suja, J. A., Santos, J. L. and Rufas, J. S. (1998). Squash procedure for protein immunolocalization in meiotic cells. *Chromosome Res.* **6**, 639-642.
Pak, J. and Segall, J. (2002). Role of Ndt80, Sum1, and Swe1 as targets of the meiotic recombination checkpoint that control exit from pachytene and spore formation in *Saccharomyces cerevisiae*. *Mol. Cell. Biol.* **22**, 6430-6440.
Parra, M. T., Viera, A., Gomez, R., Page, J., Benavente, R., Santos, J. L., Rufas, J. S. and Suja, J. A. (2004). Involvement of the cohesin Rad21 and SCP3 in monopolar attachment of sister kinetochores during mouse meiosis I. *J. Cell Sci.* **117**, 1221-1234.
Parra, M. T., Gomez, R., Viera, A., Llano, E., Pendas, A. M., Rufas, J. S. and Suja, J. A. (2009). Sequential assembly of centromeric proteins in male mouse meiosis. *PLoS Genet.* **5**, e1000417.
Perera, D., Perez-Hidalgo, L., Moens, P. B., Reini, K., Lakin, N., Syvaoja, J. E., San-Segundo, P. A. and Freire, R. (2004). TopBP1 and ATR colocalization at meiotic chromosomes: role of TopBP1/Cut5 in the meiotic recombination checkpoint. *Mol. Biol. Cell* **15**, 1568-1579.
Perez-Hidalgo, L., Moreno, S. and San-Segundo, P. A. (2003). Regulation of meiotic progression by the meiosis-specific checkpoint kinase Mek1 in fission yeast. *J. Cell Sci.* **116**, 259-271.
Petronczki, M., Siomos, M. F. and Nasmyth, K. (2003). Un menage a quatre: the molecular biology of chromosome segregation in meiosis. *Cell* **112**, 423-440.
Pittman, D. L., Cobb, J., Schimenti, K. J., Wilson, L. A., Cooper, D. M., Brignull, E., Handel, M. A. and Schimenti, J. C. (1998). Meiotic prophase arrest with failure of chromosome synapsis in mice deficient for Dmc1, a germline-specific RecA homolog. *Mol. Cell* **1**, 697-705.
Prinz, S., Amon, A. and Klein, F. (1997). Isolation of *COM1*, a new gene required to complete meiotic double-strand break-induced recombination in *Saccharomyces cerevisiae*. *Genetics* **146**, 781-795.
Rockmill, B. and Roeder, G. S. (1990). Meiosis in asynaptic yeast. *Genetics* **126**, 563-574.
Rockmill, B. and Roeder, G. S. (1991). A meiosis-specific protein kinase homolog required for chromosome synapsis and recombination. *Genes Dev.* **5**, 2392-2404.
Rockmill, B., Sym, M., Scherthan, H. and Roeder, G. S. (1995). Roles for two RecA homologs in promoting meiotic chromosome synapsis. *Genes Dev.* **9**, 2684-2695.
Roeder, G. S. (1997). Meiotic chromosomes: it takes two to tango. *Genes Dev.* **11**, 2600-2621.
Roeder, G. S. and Bailis, J. M. (2000). The pachytene checkpoint. *Trends Genet.* **16**, 395-403.
Roig, I., Dowdle, J. A., Toth, A., de Rooij, D. G., Jasin, M. and Keeney, S. (2010). Mouse TRIP13/PCH2 is required for recombination and normal higher-order chromosome structure during meiosis. *PLoS Genet.* **6,** e1001062.
Rouse, J. and Jackson, S. P. (2002). Lcd1p recruits Mec1p to DNA lesions in vitro and in vivo. *Mol. Cell* **9**, 857-869.
San-Segundo, P. A. and Roeder, G. S. (1999). Pch2 links chromatin silencing to meiotic checkpoint control. *Cell* **97**, 313-324.
San-Segundo, P. A. and Roeder, G. S. (2000). Role for the silencing protein Dot1 in meiotic checkpoint control. *Mol. Biol. Cell* **11**, 3601-3615.
Shimada, M., Nabeshima, K., Tougan, T. and Nojima, H. (2002). The meiotic recombination checkpoint is regulated by checkpoint *rad+* genes in fission yeast. *EMBO J.* **21**, 2807-2818.
Smits, V. A., Warmerdam, D. O., Martin, Y. and Freire, R. (2010). Mechanisms of ATR-mediated checkpoint signalling. *Front. Biosci.* **15**, 840-853.
Sourirajan, A. and Lichten, M. (2008). Polo-like kinase Cdc5 drives exit from pachytene during budding yeast meiosis. *Genes Dev.* **22**, 2627-2632.
Storlazzi, A., Xu, L., Schwacha, A. and Kleckner, N. (1996). Synaptonemal complex (SC) component Zip1 plays a role in meiotic recombination independent of SC polymerization along the chromosomes. *Proc. Natl. Acad. Sci. USA* **93**, 9043-9048.
Sugiyama, T. and Kantake, N. (2009). Dynamic regulatory interactions of Rad51, Rad52, and replication protein-a in recombination intermediates. *J. Mol. Biol.* **390**, 45-55.
Sym, M. and Roeder, G. S. (1994). Crossover interference is abolished in the absence of a synaptonemal complex protein. *Cell* **79**, 283-292.
Sym, M., Engebrecht, J. A. and Roeder, G. S. (1993). ZIP1 is a synaptonemal complex protein required for meiotic chromosome synapsis. *Cell* **72**, 365-378.
Tsubouchi, H. and Roeder, G. S. (2002). The Mnd1 protein forms a complex with hop2 to promote homologous chromosome pairing and meiotic double-strand break repair. *Mol. Cell. Biol.* **22**, 3078-3088.
Tsubouchi, H. and Roeder, G. S. (2003). The importance of genetic recombination for fidelity of chromosome pairing in meiosis. *Dev. Cell.* **5**, 915-925.
Tung, K. S., Hong, E. J. and Roeder, G. S. (2000). The pachytene checkpoint prevents accumulation and phosphorylation of the meiosis-specific transcription factor Ndt80. *Proc. Natl. Acad. Sci. USA* **97**, 12187-12192.
Usui, T., Ogawa, H. and Petrini, J. H. (2001). A DNA damage response pathway controlled by Tel1 and the Mre11 complex. *Mol. Cell* **7**, 1255-1266.
Viera, A., Gomez, R., Parra, M. T., Schmiesing, J. A., Yokomori, K., Rufas, J. S. and Suja, J. A. (2007). Condensin I reveals new insights on mouse meiotic chromosome structure and dynamics. *PLoS ONE* **2**, e783.
Wan, L., de los Santos, T., Zhang, C., Shokat, K. and Hollingsworth, N. M. (2004). Mek1 kinase activity functions downstream of *RED1* in the regulation of meiotic double strand break repair in budding yeast. *Mol. Biol. Cell* **15**, 11-23.
Woltering, D., Baumgartner, B., Bagchi, S., Larkin, B., Loidl, J., de los Santos, T. and Hollingsworth, N. M. (2000). Meiotic segregation, synapsis, and recombination checkpoint functions require physical interaction between the chromosomal proteins Red1p and Hop1p. *Mol. Cell. Biol.* **20**, 6646-6658.
Wu, H. Y. and Burgess, S. M. (2006). Two distinct surveillance mechanisms monitor meiotic chromosome metabolism in budding yeast. *Curr. Biol.* **16**, 2473-2479.
Xu, L., Weiner, B. M. and Kleckner, N. (1997). Meiotic cells monitor the status of the interhomolog recombination complex. *Genes Dev.* **11**, 106-118.
Yuan, L., Liu, J. G., Zhao, J., Brundell, E., Daneholt, B. and Hoog, C. (2000). The murine SCP3 gene is required for synaptonemal complex assembly, chromosome synapsis, and male fertility. *Mol. Cell* **5**, 73-83.
Zou, L. (2007). Single- and double-stranded DNA: building a trigger of ATR-mediated DNA damage response. *Genes Dev.* **21**, 879-885.
Zou, L. and Elledge, S. J. (2003). Sensing DNA damage through ATRIP recognition of RPA-ssDNA complexes. *Science* **300**, 1542-1548.

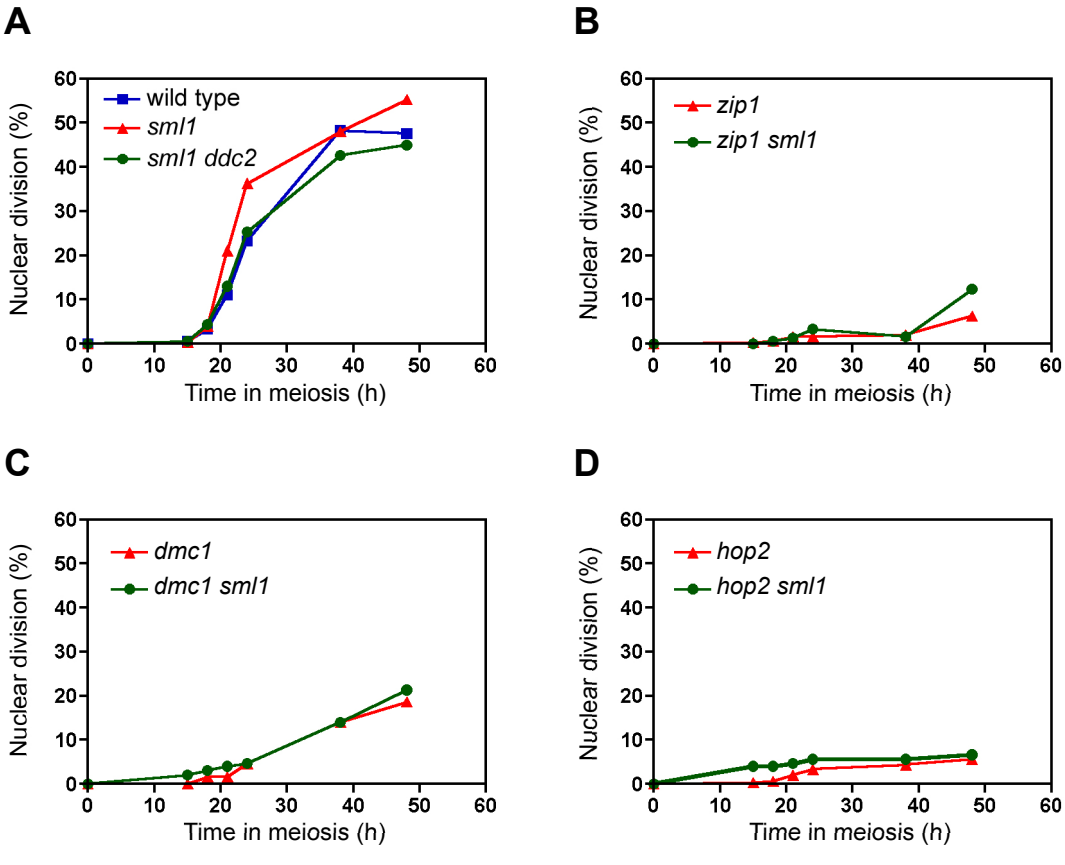
A
wild type
sml1
sml1 ddc2
Nuclear division (%)
Time in meiosis (h)
B
zip1
zip1 sml1
Nuclear division (%)
Time in meiosis (h)
C
dmc1
dmc1 sml1
Nuclear division (%)
Time in meiosis (h)
D
hop2
hop2 sml1
Nuclear division (%)
Time in meiosis (h)

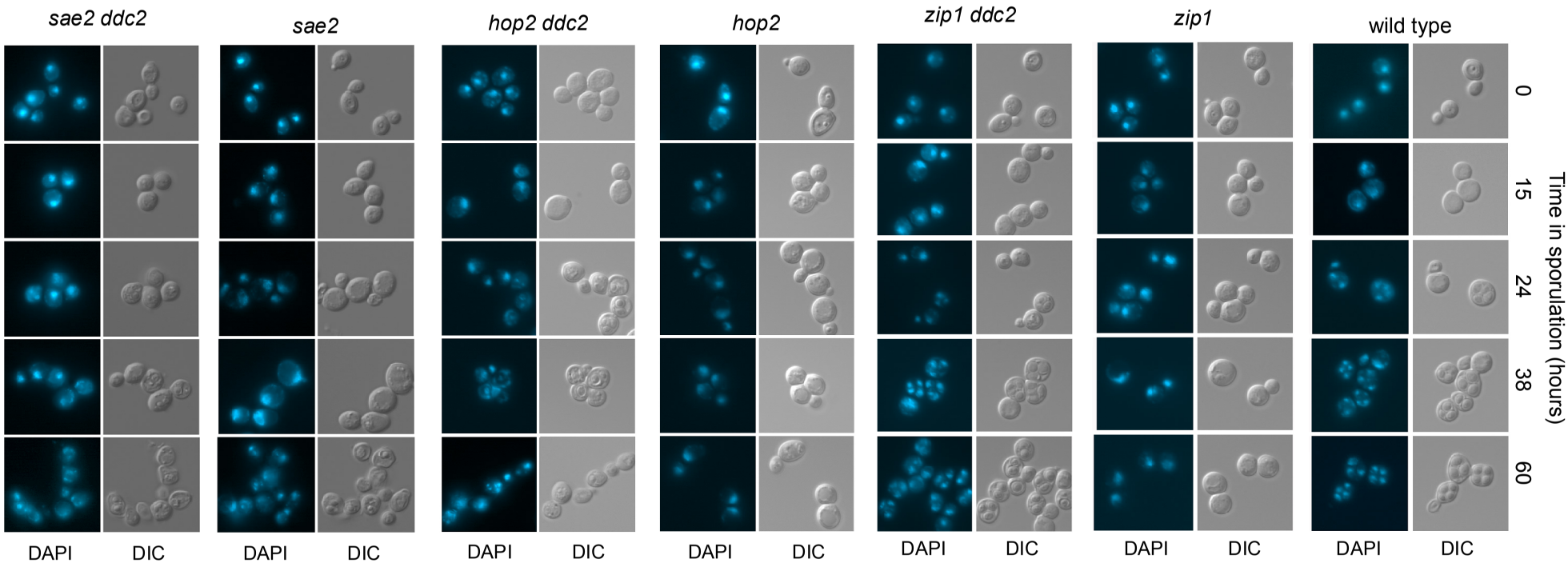
sae2 ddc2
sae2
hop2 ddc2
hop2
zip1 ddc2
zip1
wild type
DAPI
DIC
Time in sporulation (hours)
0
15
24
38
60

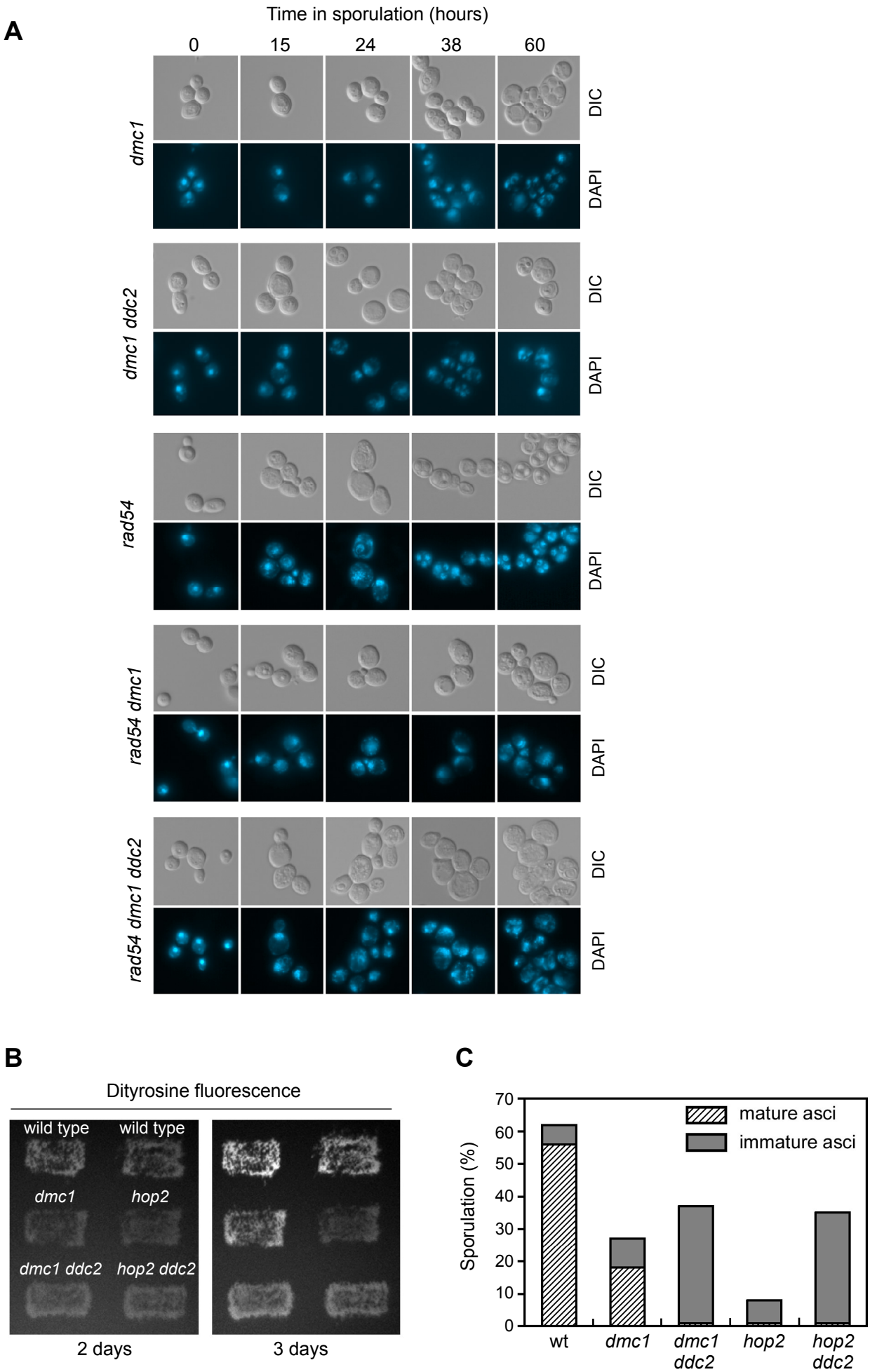
A
Time in sporulation (hours)
0
15
24
38
60
dmc1
dmc1 ddc2
rad54
rad54 dmc1
rad54 dmc1 ddc2
DIC
DAPI
B
Dityrosine fluorescence
wild type
wild type
dmc1
hop2
dmc1 ddc2
hop2 ddc2
2 days
3 days
C
Sporulation (%)
mature asci
immature asci
wt
dmc1
dmc1 ddc2
hop2
hop2 ddc2

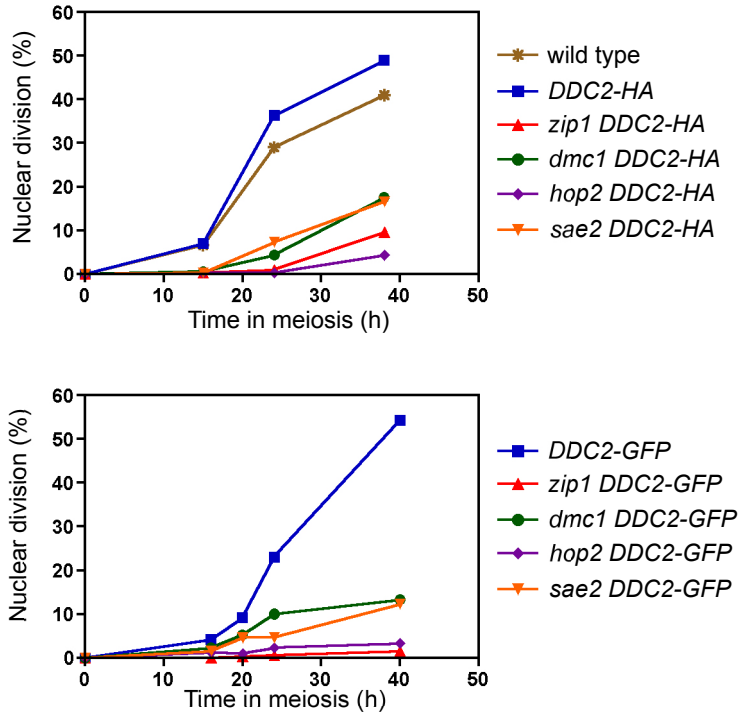
Nuclear division (%)
Time in meiosis (h)
0
10
20
30
40
50
60
wild type
DDC2-HA
zip1 DDC2-HA
dmc1 DDC2-HA
hop2 DDC2-HA
sae2 DDC2-HA
DDC2-GFP
zip1 DDC2-GFP
dmc1 DDC2-GFP
hop2 DDC2-GFP
sae2 DDC2-GFP

A

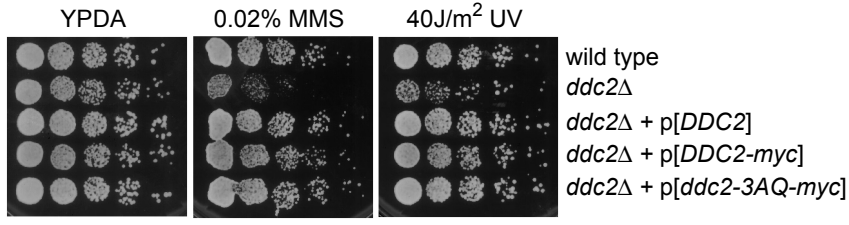
YPDA
0.02% MMS
40J/m2 UV
wild type
ddc2Δ
ddc2Δ + p[DDC2]
ddc2Δ + p[DDC2-myc]
ddc2Δ + p[ddc2-3AQ-myc]

B

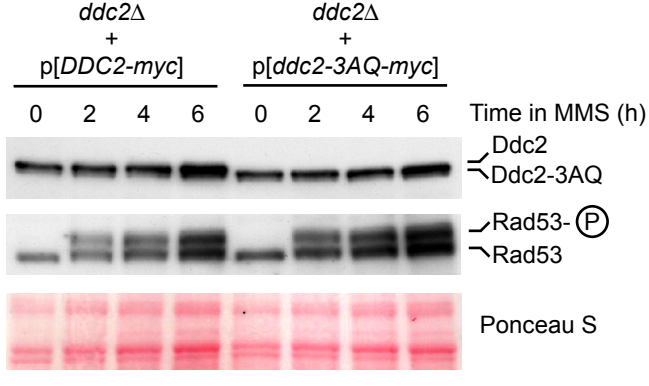
ddc2Δ + p[DDC2-myc]
ddc2Δ + p[ddc2-3AQ-myc]
0 2 4 6 0 2 4 6
Time in MMS (h)
Ddc2
Ddc2-3AQ
Rad53-P
Rad53
Ponceau S

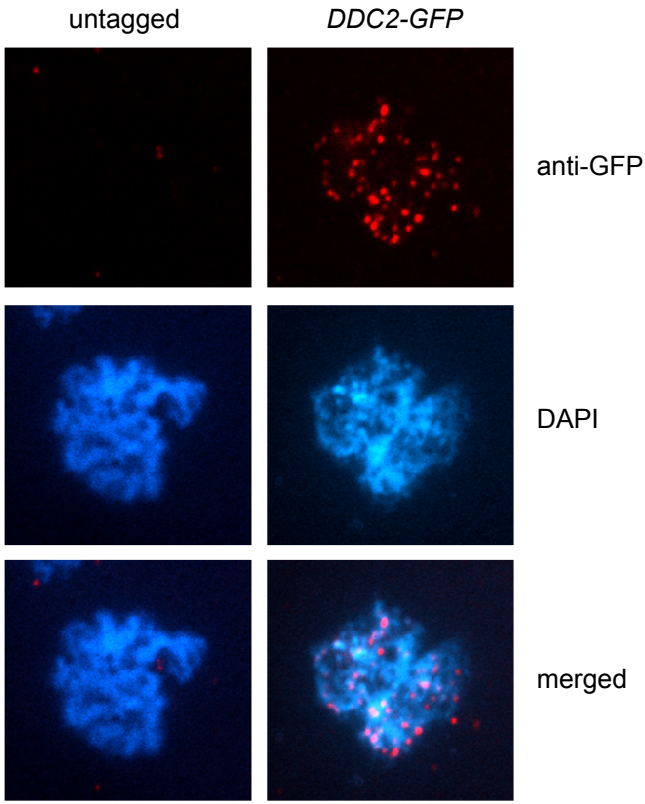
untagged
DDC2-GFP
anti-GFP
DAPI
merged
dmc1

A

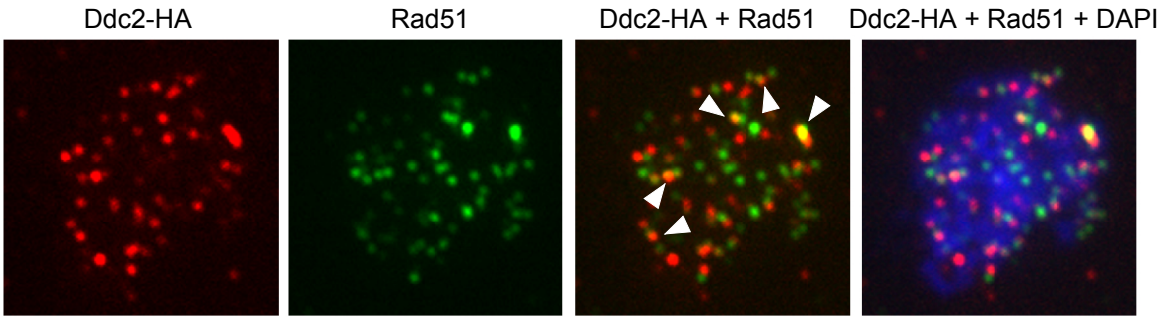

hop2 mutant

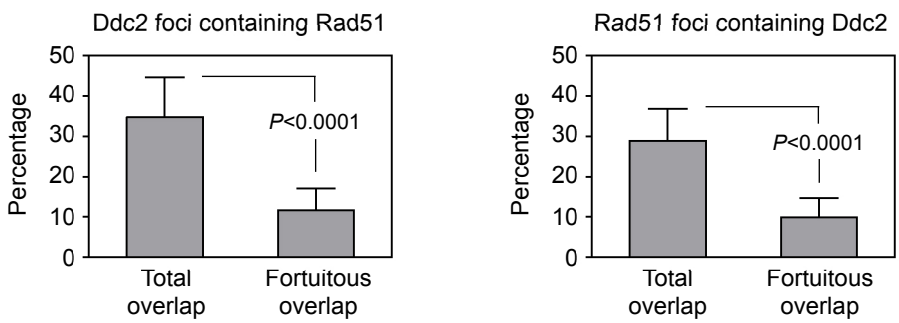

B

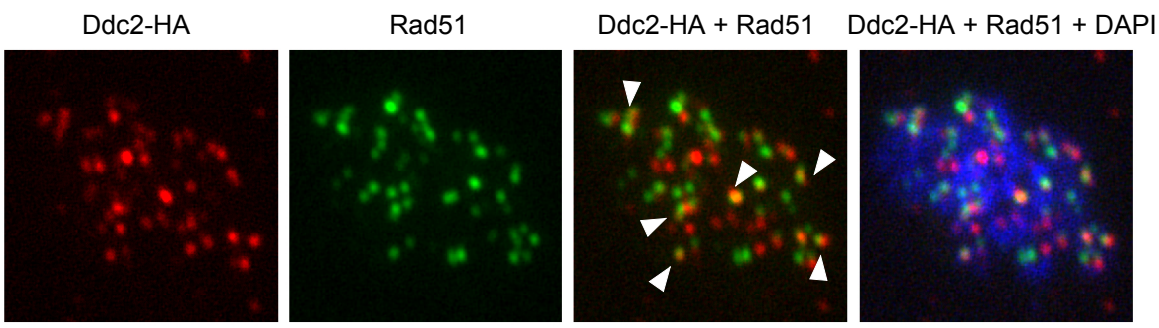

dmc1 mutant

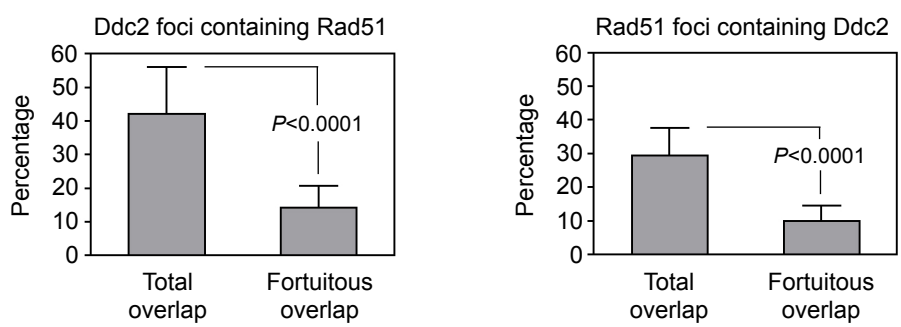

Table S1. *Saccharomyces cerevisiae* strains

Strain	Genotype*
BR1919-2N	*MAT***a**/*MATα leu2-3,112 his4-260 ura3-1 ade2-1 thr1-4 trp1-289*
DP421	BR1919-2N *lys2ΔNheI*
DP422	DP421 *zip1::LYS2*
DP448	DP421 *DDC2-GFP::TRP1*
DP449	DP421 *zip1::LYS2 DDC2-GFP::TRP1*
DP450	DP421 *dmc1::kanMX6 DDC2-GFP::TRP1*
DP451	DP421 *sml1::kanMX6 zip1::LYS2 ddc2::TRP1*
DP452	DP421 *sml1::kanMX6 zip1::LYS2*
DP454	DP421 *sml1::kanMX6 ddc2::TRP1*
DP455	DP421 *sml1::kanMX6*
DP456	DP421 *dmc1::kanMX6*
DP465	DP421 *spo11::ADE2 DDC2-GFP::TRP1*
DP466	DP421 *spo11::ADE2 dmc1::kanMX6*
DP467	DP421 *sml1::kanMX6 dmc1::kanMX6*
DP468	DP421 *sml1::kanMX6 dmc1::kanMX6 ddc2::TRP1*
DP469	DP421 *spo11::ADE2 dmc1::kanMX6 DDC2-GFP::TRP1*
DP470	DP421 *hop2::LEU2*
DP471	DP421 *sml1::kanMX6 hop2::LEU2*
DP472	DP421 *sml1::kanMX6 hop2::LEU2 ddc2::TRP1*
DP473	BR1919-2N *sml1::kanMX6 rad54::LEU2*
DP475	BR1919-2N *sml1::kanMX6 rad54::LEU2 dmc1::hphMX4 lys2ΔNheI/LYS2*
DP480	DP421 *hop2::LEU2 DDC2-GFP::TRP1*
DP481	DP421 *sml1::kanMX6 rad54::LEU2 dmc1::hphMX4 ddc2::TRP1*
DP484	DP421 *sae2::kanMX6 DDC2-GFP::TRP1*
DP485	DP421 *sml1::kanMX6 sae2::kanMX6*
DP487	DP421 *DDC2-3HA::kanMX6*
DP488	DP421 *dmc1::kanMX6 DDC2-3HA::kanMX6*
DP489	DP421 *sml1::kanMX6 sae2::kanMX6 ddc2::TRP1*
DP490	DP421 *zip1::LYS2 DDC2-HA::kanMX6*
DP491	BR1919-2N *hop2::LEU2 DDC2-3HA::kanMX6 LYS2/lys2ΔNheI*
DP492	DP421 *sae2::kanMX6 DDC2-3HA::kanMX6*

DP608	DP421 *dmc1::hphMX4 DDC2-GFP::TRP1 BrdU-Inc::URA3/ura3-1*
DP693	DP421 *ndt80::LEU2 dmc1::kanMX6 DDC2-3HA::kanMX6*
DP695	DP421 *ndt80::LEU2 dmc1::kanMX6 spo11::ADE2 DDC2-3HA::kanMX6*
DP697	DP421 *SPO11-GFP::kanMX6 DDC2-3HA::kanMX6*
DP778	DP421 *sml1::kanMX6 TUB1-GFP::TRP1/TUB1*
DP779	DP421 *sml1::kanMX6 dmc1::KanMX6 TUB1-GFP::TRP1/TUB1*
DP780	DP421 *sml1::kanMX6 hop2::LEU2 TUB1-GFP::TRP1/TUB1*
DP781	DP421 *sml1::kanMX6 dmc1::KanMX6 ddc2::hphMX4 TUB1-GFP::TRP1/TUB1*
DP782	DP421 *sml1::kanMX6 hop2::LEU2 ddc2::hphMX4 TUB1-GFP::TRP1/TUB1*
YP1027	BR1919**a** *ddc2::TRP1 lys2ΔNheI* [pLCD1-myc (*URA3*)]
YP1028	BR1919**a** *ddc2::TRP1 lys2ΔNheI* [pSS136 (*URA3*)]
W303-2N	*MAT***a**/*MAT*α *leu2-3,112 trp1-1 ura3-1 ade2-1 his3-11,15 can1-100 rad5-G535R*
DP433	W303-2N *sml1::URA3 DDC2-GFP::TRP1*
DP434	W303-2N *sml1::URA3 dmc1::kanMX6 DDC2-GFP::TRP*
DP505	W303-2N *rfa1-t11 dmc1::kanMX6 DDC2-GFP::TRP1*
DP506	W303-2N *rfa1-t11 DDC2-GFP::TRP1*

*Unless indicated, all diploid strains are homozygous for the markers.